Electronic, Magnetic, and Thermal properties of $Pb_{2-x}A_xCrO_5$ (A = K or La)

Biljana Indovski, B.Sc.

Physics Program

Submitted in partial fulfillment
of the requirements for the degree of

Master of Science in Physics

Faculty of Mathematics and Sciences, Brock University
St. Catharines, Ontario

Abstract

Lead chromium oxide is a photoconductive dielectric material that has great potential of being used as a room temperature photodetector. In this research, we made ceramic pellets of this compound as well as potassium doped compound $Pb_{2-x}K_xCrO_5$, where x=0, 0.05, 0.125. We also investigate the properties of the lanthanum doped sample whose chemical formula is $Pb_{1.85}La_{0.15}CrO_5$. The electronic, magnetic and thermal properties of these materials have been studied. Magnetization measurements of the Pb_2CrO_5 sample indicate a transition at about 310 K, while for the lanthanum doped sample the transition temperature is at about 295 K indicating a paramagnetic behavior. However, the potassium doped samples are showing the transition from paramagnetic state to diamagnetic state at different temperatures for different amounts of potassium atoms present in the sample. We have studied resistivity as a function of temperature in different gas environments from 300 K to 900 K. The resistivity measurement of the parent sample indicates a conducting to insulating transition at about 300 K and upon increasing the temperature further, above 450 K the sample becomes an ionic conductor. As temperature increases a decrease in resistance is observed in the lanthanum/potassium doped samples. Using Differential Scanning Calorimetry experiment an endothermic peak is observed for the Pb_2CrO_5 and lanthanum/ potassium doped samples at about 285 K.

Contents

List of Tables

List of Figures

Acknowledgements

I would like to thank everybody that had helped me during this research, especially to the members of my committee Dr. Shyamal K. Bose, Dr. Maureen Reedyk, and my supervisor Dr. Fereidoon S. Razavi. Dr. Razavi is a wonderful teacher and supervisor and from his guidance I have learned many skills.

Also I would like to thank Dr. Thad A. Harroun for his advice and for allowing me to run DSC measurements, and Drew Marquart for his assistance in conducting these experiments.

Thanks to Dr. Mangala Singh and Dr. Reza Mohammadizadeh for the productive discussions and their help during this research.

I had great help from the Machine shop, Electronic shop and the Glass blowers and I would like to thank them for that.

Thanks to the whole Physics Department, all the faculty members and all the students for making this experience as significant and memorable as it should be.

At the end I would like to thank my husband and my parents for giving me strong support and encouragement in these two years.

Chapter 1

Introduction

Lead chromium oxide is a dark red mineral with yellowish-orange streaks (see figure 1.1). This mineral, also known as a phoenicochroite, was first discovered in 1839 in the Ural Mountains, in Russia. It is a massive mineral with hardness of 2.5 on the Mohs scale and has a polycrystalline morphology [1, 5]. Intensive research on the optical properties of this material has been done in the past. Ceramic samples of Lead chromium oxide were fabricated by a solid state solution technique and the material was found to be dielectric [6].

Photoconductivity was observed in the visible region in the ceramic sample. In the measurements of the photocurrent as a function of applied voltage a decrease in resistance was observed with an increase of light intensity. Due to its center of symmetry the photoconductive response in this compound is not the same as the one observed in the ferroelectric materials [7].

A photovoltaic effect was also observed in Pb_2CrO_5 ceramic samples. The simple photovoltaic device is the Pb_2CrO_5 ceramic sample with pair of planar electrodes, usually an Au/Au, Au/Al, Al/Al or Ag/Ag combination. The planar electrodes were evaporated on one surface of the ceramic sample and as a light source a projector tungsten lamp was used. When the Pb_2CrO_5 photovoltaic device was illuminated, the voltage was measured as a potential difference between two points: one on each of the electrodes. From the experimental results it was concluded that the photovoltaic effect in Pb_2CrO_5 devices with the Au or Ag electrodes is a result of the excitation

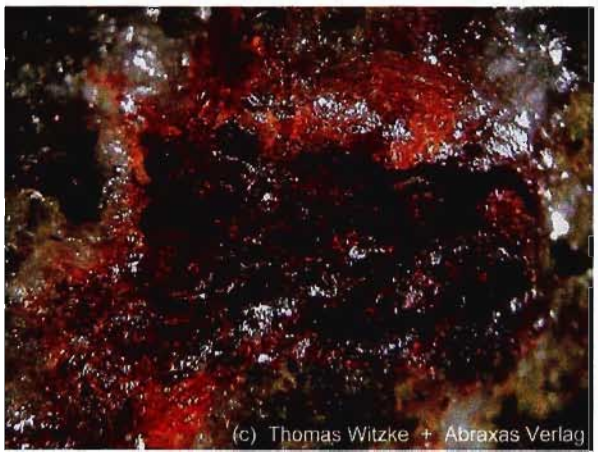

Figure 1.1: **Phoenicochroite mineral,** [1]

of the electrons by light absorption in the metal electrode and the presence of the Schottky barrier on the metal-semiconductor interface [8].

Thin films of Pb_2CrO_5 have been fabricated using an Electron Beam Evaporation technique on a glass substrate. The measured photovoltage in these thin films had a greater value than the one measured in the ceramic samples. The optical transmission and reflectance were measured and this data was used to calculate the absorption constant and it was found that the band-gap energy is about 2.3-2.4 eV [9].

Also, Pb_2CrO_5 thin films were prepared with different substrate temperatures that caused their structure to crystallize in different preferred orientations. The color of the thin films also differed depending on the substrate temperature. Annealing of the thin film samples improves the crystallization of the samples and the color becomes orange as expected [10].

Furthermore, the photoconductive effect was studied on the Pb_2CrO_5 thin films with planar electrodes, as described above. Also, the photoconduction of the thin film was measured when electrodes were in interdigital arrangement. Interdigital electrodes are two planar electrodes that are deposited on the sample and between

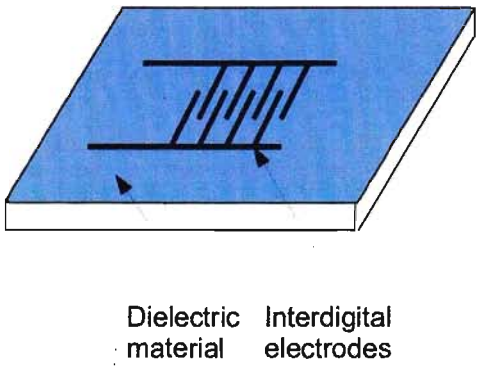

Figure 1.2: **Interdigital electrodes**

them fingers are deposited using an electron-beam lithography technique. An example is shown in figure 1.2. The electrodes arrangement affects the photoconductivity of the thin films substantially. The band gap of Pb_2CrO_5 thin films was determined from the spectral photoconductive response to be between 2.2-2.4 eV in the visible region [11, 12].

An important application of Pb_2CrO_5 is as a position sensitive photodetector. These devices are semiconductors with interdigital electrodes such that when illuminated a photocurrent is produced. This photocurrent is converted to an output voltage that is being measured as a function of the light beam position. Lead chromium oxide position sensitive photodetector is applicable in the visible and near-ultraviolet regions [13].

Also, due to its sensitivity in the UV region, Pb_2CrO_5 has a potential application as an UV radiation intensity measuring device, and as an UV and visible light detecting device [11].

The goal of this research is to investigate the electronic, magnetic and thermal properties of the Pb_2CrO_5 and La or K doped samples. In Chapter 2 of this thesis the crystal structure and the sample preparation of $Pb_{2-x}A_xCrO_5$ (A=K or La), are described. In Chapter 3 the details of the experimental techniques used to deter-

mine the structural, electronic, magnetic and thermal properties of these samples are described. Also in this chapter the experimental results are presented followed by discussion. The conclusions are summarized in the final chapter.

Chapter 2

Structural Properties and Sample Preparation

2.1 Crystal Structure of Pb_2CrO_5

The crystal structure of Pb_2CrO_5 is monoclinic with space group C2/m (C-single-face centered lattice, m-mirror plane). There are 4 molecules in the unit cell and therefore there are 8 atoms of Lead, 4 atoms of Chromium, and 20 Oxygen atoms total in one unit cell. One Chromium atom and four Oxygen atoms that are marked as O1, O2, and O3 in figure 2.1 form the $(CrO_4)^{2-}$ tetrahedron. The fifth Oxygen atom marked as O4 in figure 2.1 is coordinated by four Lead atoms, marked as Pb1 and Pb2, and forms an OPb_4 tetrahedron [2]. In this research we are doping Pb_2CrO_5 with K or La atoms. The lattice parameters for the Pb_2CrO_5, $Pb_{1.95}K_{0.05}CrO_5$, $Pb_{1.875}K_{0.125}CrO_5$, and $Pb_{1.85}$ $La_{0.15}CrO_5$ samples were calculated using the software UnitCell and the data from the X-ray powder diffraction [14]. These results are compared with the data from the PDF card for the Pb_2CrO_5, C2/m space group [15] in table 2.1. The results for the K doped samples reveal that the volume of the unit cell increases as the amount of K atoms increases. The lattice parameters a and β are larger, c is slightly smaller and b is almost the same as the data for the space group C2/m. For the sample doped with La, the size of the unit cell significantly increases. Compared to the parameters of the sample with space group C2/m, b and c are larger, a and β

	Pb_2CrO_5	$Pb_{1.95}K_{0.05}CrO_5$	$Pb_{1.875}K_{0.125}CrO_5$	$Pb_{1.85}\ La_{0.15}CrO_5$	Pb_2CrO_5 [15]
a(Å)	13.972	13.993	14.113	13.898	14.02
σ(Å)	0.001	0.001	0.001	0.001	
b(Å)	5.675	5.688	5.682	5.775	5.68
σ(Å)	0.001	0.001	0.001	0.001	
c(Å)	7.164	7.132	7.113	7.172	7.14
σ(Å)	0.001	0.001	0.001	0.001	
β(°)	115.278	115.260	115.121	114.638	115.23
σ(°)	0.006	0.005	0.006	0.005	
V(Å^3)	513.68	513.33	516.41	523.16	514.76
σ(Å^3)	0.05	0.04	0.06	0.04	

Table 2.1: Lattice parameters

are smaller. This indicates that substitution of La atoms in place of Pb atoms causes a significant increase in the volume of the unit cell. The results are presented with error that has been obtained from the calculation program Unit Cell where estimated error used for 2θ was 0.005 °. Having an anion $(CrO_4)^{2-}$ formed in the structure, the valence of the atoms in Pb_2CrO_5 are Pb^{2+}, Cr^{6+} and O^{2-} [6]. If impurities are introduced there will be excess of carriers in the sample. When Pb^{2+} atoms are replaced with La^{3+}, the sample is doped with electrons. This sample will have a mixture of Cr^{6+} ($3d^0$), Cr^{3+} ($3d^3$), Cr^{2+} ($3d^4$) ions. When sample is doped with K^{1+} atoms the valence of Pb atom changes and Pb^{2+} ($5d^{10}6s^2$), Pb^{4+} ($5d^{10}$) ions are present in the structure. These samples are doped with holes.

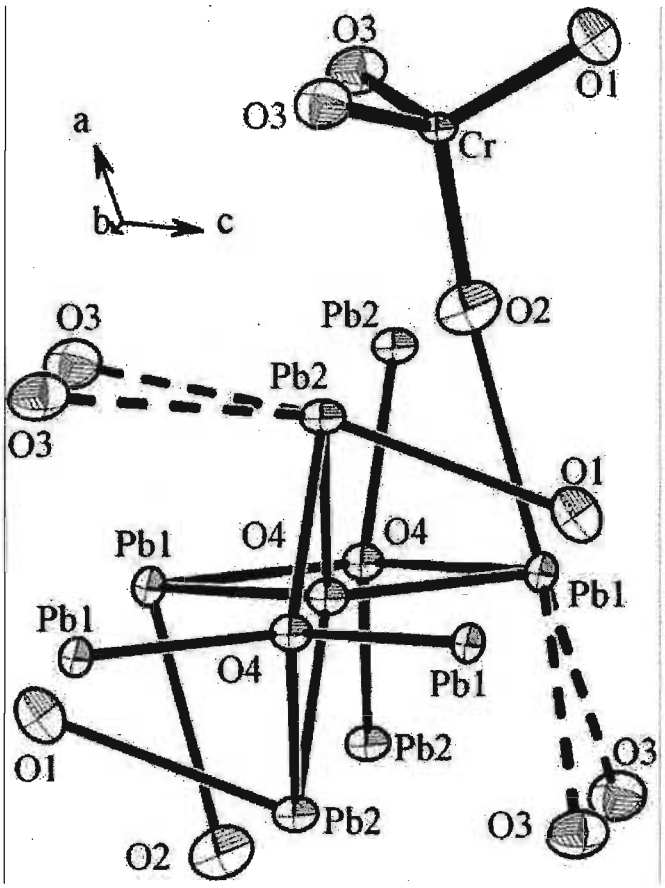

Figure 2.1: **Crystal structure of Pb_2CrO_5 ceramic sample [2]**

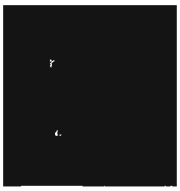

Figure 2.2: **Pb_2CrO_5 ceramic sample**

2.2 Sample Preparation

2.2.1 Ceramic sample

Experimental method

The preparation of the ceramic pellets of $Pb_{2-x}K_xCrO_5$ was done by using a solid state solution technique previously applied by Dr. Koffyberg[1]. The starting materials were powders and used as they were purchased: PbO, $Cr(NO_3)_3 \cdot yH_2O$ and K_2CO_3. A calculated amount of each compound was placed in a quartz crucible and approximately 50 ml distilled water was added to the mixture. A quartz crucible was used to avoid reaction with the sample which had occurred when an aluminum oxide crucible was used. The crucible was heated on a hot plate until the water evaporated. This step was done to drive off nitrate. Then the crucible was placed in a heated furnace at 500 °C for 24h. Samples were cooled down in the room environment and material was collected and grounded with acetone using mortar and pestle until the acetone evaporates. Pellets were made under 6 tons of pressure and heated in a furnace at 650 °C for 72h. Again, the cooling down was done in the room environment. Pellets were a dark red color as it can be seen from figure 2.2 and this color was expected (see figure 1.1).

[1]Dr. Koffyberg was a Brock University professor who had prepared samples for research

Stoichiometry calculation

In order to calculate the correct amounts of each material, first the chemical equation must be balanced. The balanced chemical equation for Pb_2CrO_5 sample is:

$$2PbO + Cr(NO_3)_3 \cdot yH_2O + H_2O \longrightarrow Pb_2CrO_5 + vapor + gas \tag{2.1}$$

The balanced chemical equation for $Pb_{2-x}K_xCrO_5$ sample is:

$$(2-x)PbO + Cr(NO_3)_3 \cdot yH_2O + \frac{x}{2}K_2CO_3 + H_2O \longrightarrow Pb_{2-x}K_xCrO_5 + vapor + gas \tag{2.2}$$

The next step is calculating the correct amount of each material. For example, to make Pb_2CrO_5 first a calculation of the molar mass for PbO and $Cr(NO_3)_3 \cdot 9H_2O$ is done. The molar mass for PbO is:

$$207.2 + 15.9994 = 223.2g/mol \tag{2.3}$$

The molar mass for $Cr(NO_3)_3 \cdot 9H_2O$ is:

$$51.996 + 3 \cdot (14.0067 + 3 \cdot 15.9994) + 9 \cdot (2 \cdot 1.0079 + 15.9994) = 400.15g/mol \tag{2.4}$$

The correct masses of the reactants are:

For PbO: $(2 \cdot 223.2)/100 = 4.464$ g

For $Cr(NO_3)_3 \cdot 9H_2O$: $400.15/100 = 4.0015$ g.

When the information for the amount of water was not given ($Cr(NO_3)_3 \cdot yH_2O$) then the calculation was different. Using the information given that there is 12.7 % of Chromium in $Cr(NO_3)_3 \cdot yH_2O$, first we need to calculate the necessary amount of Chromium and then we can calculate the total mass needed, by using the following equation:

$$m_t = \frac{m_c}{0.127} \tag{2.5}$$

where m_t is the total mass, m_c is the mass of chromium. Lanthanum doped sample $Pb_{1.85}\ La_{0.15}CrO_5$, was prepared using the same experimental method.

2.2.2 Thin film

Pulsed Laser Deposition Technique

Pulsed Laser Deposition is a technique used for production of thin films that uses laser pulses as an energy source and a vacuum chamber where the deposition is done. The vacuum chamber houses a substrate holder and a target holder. An example of this kind of set-up is shown in figure 2.3 [16]. The laser beam is directed toward the rotating target by use of lenses and mirrors, and the substrate is placed in a substrate holder under the target. The substrate holder is surrounded by a heating element. When pulses are hitting the target a plume of particles is created and that is how the material is transferred to the surface of the substrate.

For the laser we used a COMPexPro 201/205 that uses 4 types of gases to operate: halogen (Fluorine gas, F_2), rare (Krypton gas, Kr), buffer (Neon gas, Ne), and inert (Helium gas, He). This laser produces light with 248 nm wavelength. When the laser is operated externally the following information is entered:

1. pulse width, the duration of the pulse;
2. pulse interval, the time between pulses;
3. number of pulses, the frequency or repetition of the pulses.

A very important safety measure is having proper eye protection since the laser beam is not passing through a completely sealed path [17].

Pb_2CrO_5 thin film

To prepare Pb_2CrO_5 thin films, Pyrex glass substrates were used. K. Toda et al. have successfully produced thin films of Pb_2CrO_5 on glass substrates using an Electron-Beam Evaporation technique [10]. In this thesis the thin films of Pb_2CrO_5 are denoted as Pb_2CrO_5-n, where n is different number for different film. To prepare Pb_2CrO_5-1

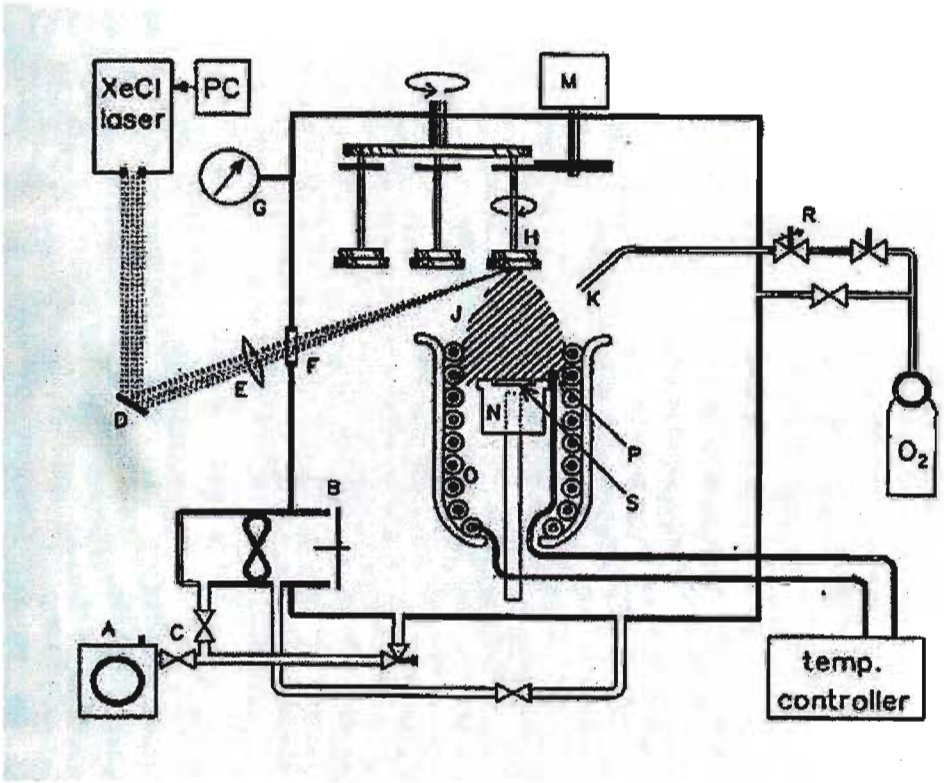

Figure 2.3: **Growth chamber, A is a roughing pump, B is turbo pump, D is a reflecting mirror, E-lens, F-quartz window, H-rotating target, J-plume of particles, S-substrate, N-substrate holder, O-heating element, P-thermometer**

thin film, in the chamber O_2 gas was under pressure of 0.300 mbar. The temperature of the substrate was 350 °C and the beam energy was 508 mJ. Pulse width was 0.05 s, pulse interval was 0.4 s, and the number of pulses 7500. After deposition the film was cooled down at a rate of 150 °C/hour in O_2 gas at 0.300 mbar. The color of the film was bright orange as expected [10]. The crystal structure of the film was investigated by X-ray Diffraction (see figure 2.10). The Pb_2CrO_5-3 thin film was made under similar conditions as Pb_2CrO_5-1. The temperature of the substrate was 350 °C, the pressure was 0.297 mbar in O_2 gas, the beam energy was 447 mJ, but after deposition the film was annealed for 1.5 h at 450 °C. The color of this film was also orange but with more intensity and the crystal structure of this film was also investigated by X-ray Diffraction (see figure 2.11).

2.3 Energy Dispersive X-ray Analysis

Energy Dispersive X-ray Analysis (EDX) or Energy Dispersive Spectroscopy (EDS) is a technique used for determination of the constituent atoms in compounds. In this technique a focused electron beam is used to scan over the surface of the sample. The beam electrons collide with the electrons that are in the atomic orbits and this causes some of the electrons to be knocked out and the atom becomes unstable. For the atom to become stable again an electron from higher energy level has to replace the empty position of the knocked out electron and as a result an X-ray photon is emitted. This X-ray photon is characteristic for each element. If an electron from a K shell is knocked out and an electron from an L shell replaces it, then a K_α X-ray is emitted, but if it is an electron from an M shell that replaces the knocked out electron from the K shell, then a K_β X-ray is emitted (see figure 2.4). The emitted X-rays are detected and displayed on a cathode ray tube screen. Further, this type of data

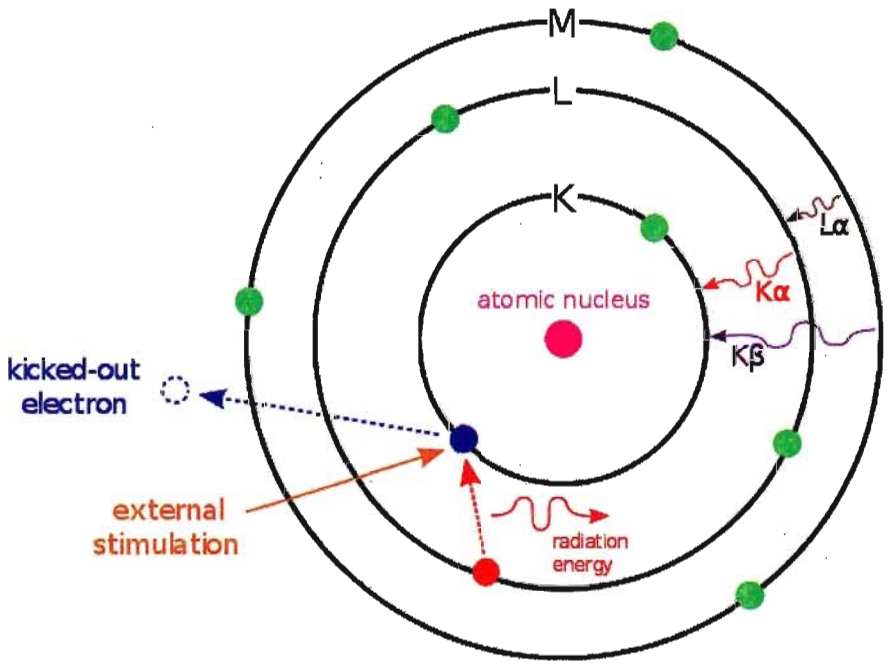

Figure 2.4: **EDS technique** [3]

can be used to form high resolution images, a technique called Scanning Electron Microscopy, SEM [18].

Experimental Results

The EDS result for the Pb_2CrO_5 sample is given in figure 2.5. The lead atoms are detected from the Pb-M_α, Pb-L_α, and Pb-$L_{\beta 1}$ peaks and Chromium atoms from the Cr-K_α and Cr-K_β peaks. The EDS result for the $Pb_{1.95}K_{0.05}CrO_5$ ceramic sample is shown in figure 2.6. In this result we can notice the presence of Pb, and Cr atoms but also the presence of K atoms and that is from the peak K-K_α. The small presence of Si atoms could be from the quartz crucible that was used in the sample preparation. The presence of the Al and Cu atoms could be a result of the equipment used in these experiments.

The figures 2.7 and 2.8 show SEM images of the surface of the Pb_2CrO_5 ceramic

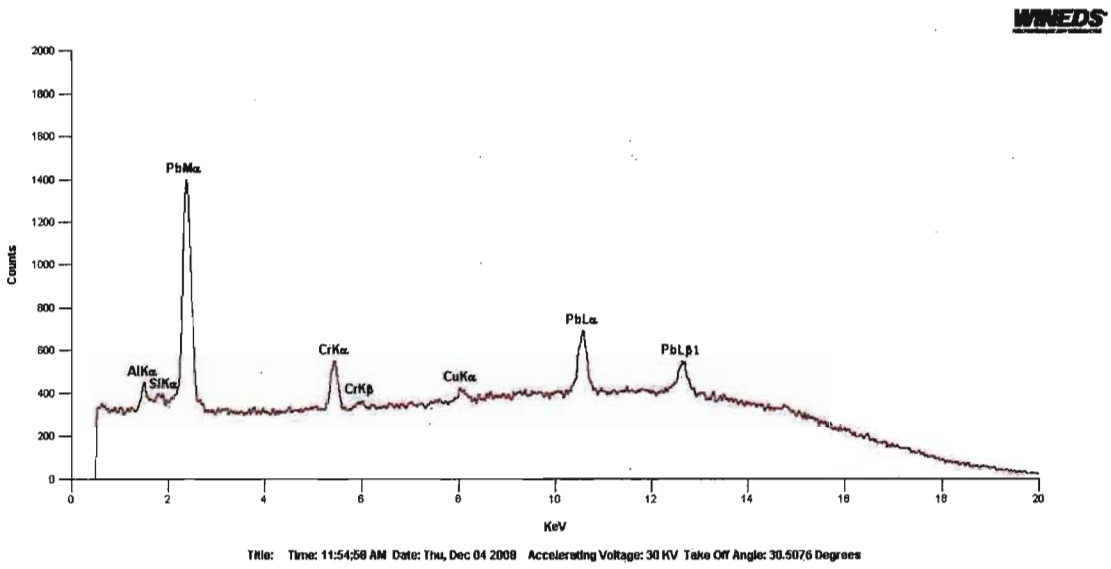

Figure 2.5: **EDS result for Pb_2CrO_5 ceramic sample**

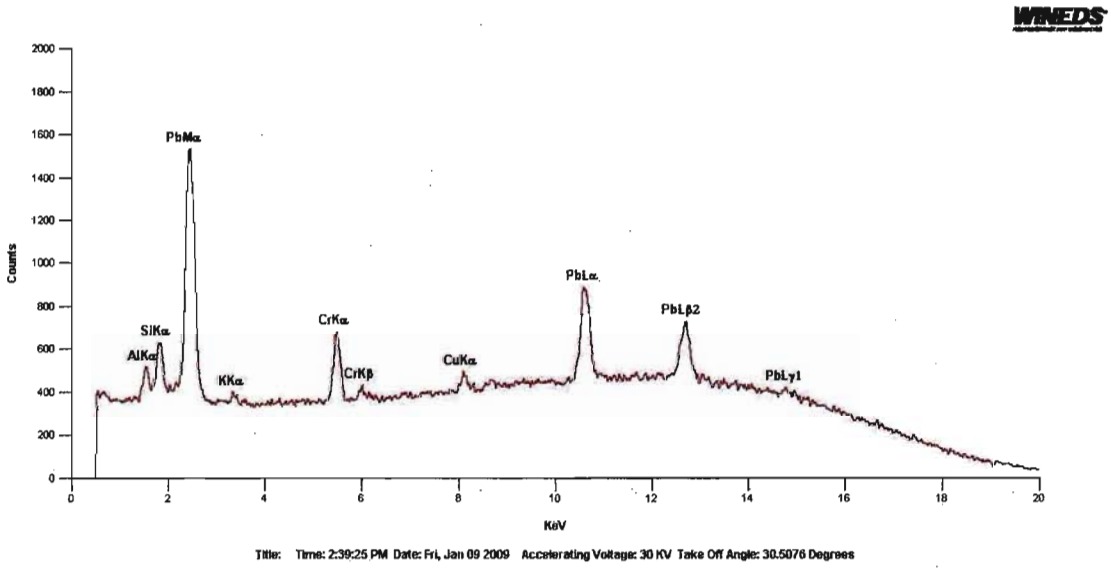

Figure 2.6: **EDS result for $Pb_{1.95}K_{0.05}CrO_5$ ceramic sample**

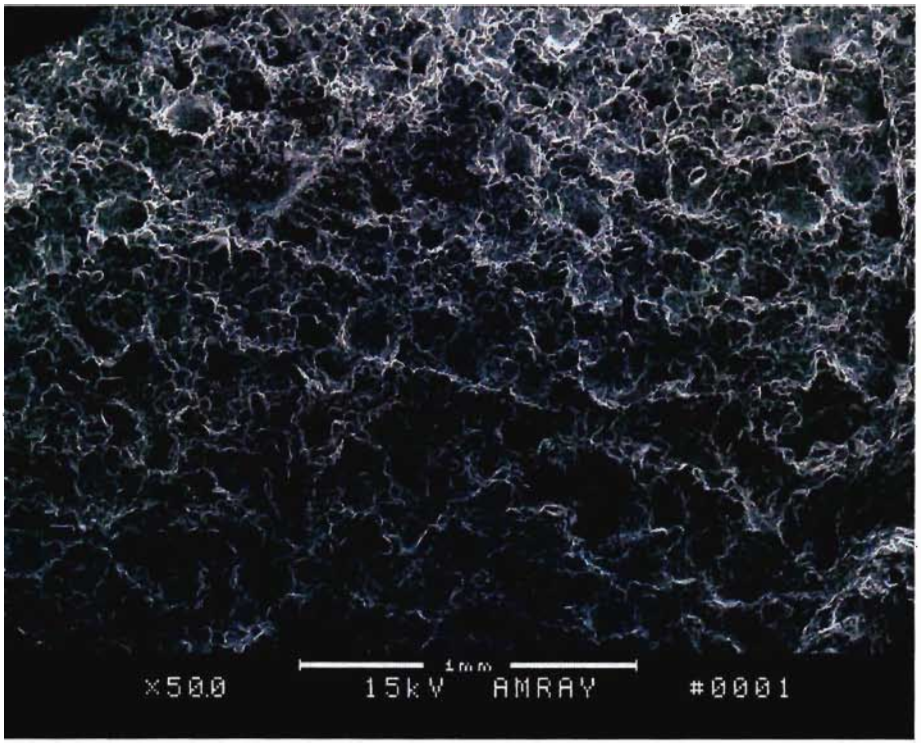

Figure 2.7: **SEM result for Pb_2CrO_5 ceramic sample, resolution 50x**

sample. From these pictures we can see the surface of the sample in two different resolutions. In figure 2.7 we can note the presence of vacancies on the surface of the sample.

2.4 X-ray Diffraction Technique

To determine the crystal structure of the samples we use the X-ray Diffraction technique. In this technique X-rays are incident on the sample and most of the rays are passing through but some are diffracted. Since the structure of a compound is composed of many parallel planes therefore the x-rays are reflected not just from the surface layer but from many planes. The net reflection will be weak for most of the incident angles because the reflected rays are out of phase. There are a few specific

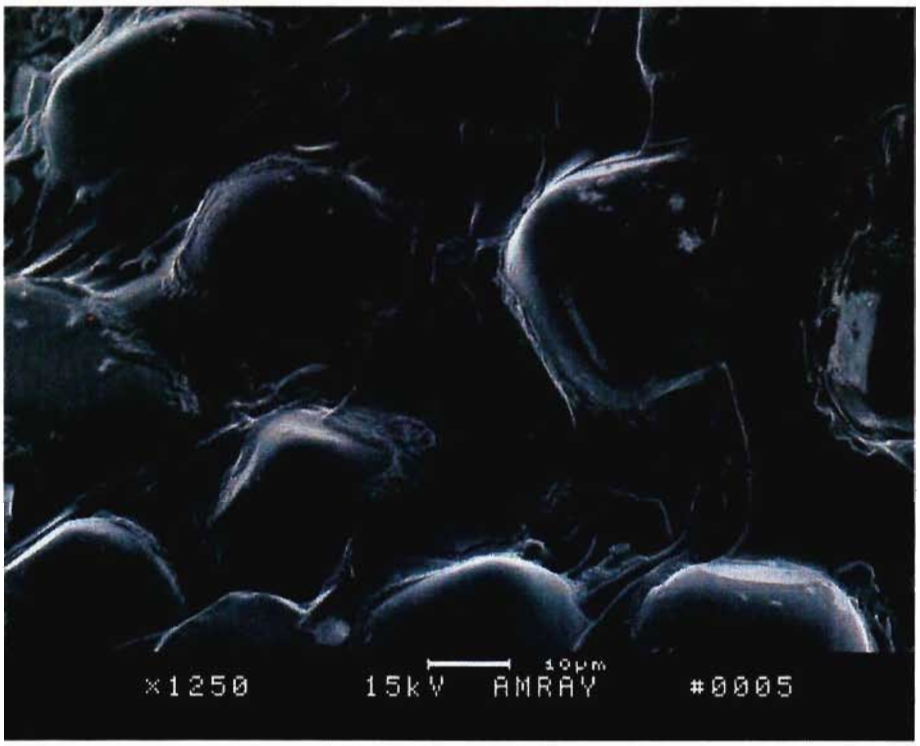

Figure 2.8: **SEM result for Pb_2CrO_5 ceramic sample, resolution 1250x**

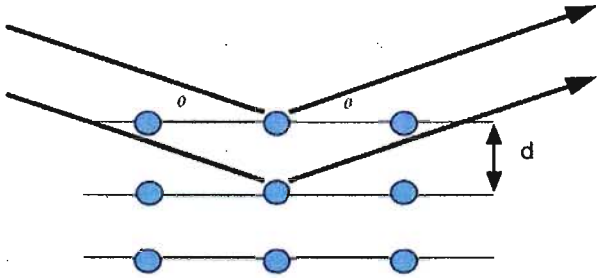

Figure 2.9: **Bragg's law**

angles for which the reflected rays are in phase which results in a strong net reflection. This reflection is called X-ray diffraction. The Bragg's condition that can be derived from the geometry shown in figure 2.9 is given with the equation 2.6:

$$m \cdot \lambda = 2 \cdot d \cdot sin\theta \tag{2.6}$$

In this equation λ is the wavelength of the X-rays, d is the distance between the atomic planes, θ is the incident angle and m is an integer number. When the angle of incidence θ satisfies the Bragg's condition the X-ray will reflect from the sample [19].

In this experiment we use a CuK_α tube that is powered with 30 kV and 20 to 30 mA of current. The ceramic sample is mounted on the sample holder using two sided tape. We use a small microscope with a scale to align the surface of the sample to be at zero on the scale. After placing the sample holder with the aligned sample on the goniometer we maximize the intensity for the main peak at fixed values for 2θ and Ω by adjusting the values for κ and ϕ, and also by moving the sample backwards and forwards. Here, Ω is the angle between the plane of the sample and the detector, that is half of 2θ, κ is the angle for which the sample rotates around its horizontal axis that is parallel to the sample surface on which the X-rays are incident. ϕ is the angle for which sample can rotate around its vertical axis. Once the intensity for the main reflection peak is maximized we can measure the intensity of the reflections for more angles.

2.4.1 Experimental Results

Thin film

The crystal structure of the Pb_2CrO_5-1 and Pb_2CrO_5-3 thin films has been investigated by using the X-ray Diffraction technique. From figure 2.10 we can detect the two main peaks (310) and ($\bar{4}02$) and ($\bar{1}12$) that are characteristic for the Pb_2CrO_5 ceramic sample, but we also observe many other peaks characteristics for this structure [15]. We can conclude that the morphology of the crystal structure of thin film Pb_2CrO_5-1 is polycrystalline. Also we can note that when 2θ is near 22 ° there is a peak that could be a result of the glass substrate, as is the increase in the intensity in the background in the area for 2θ from 15 ° to 35 °. This has been confirmed when X ray diffraction was done on a glass substrate as shown in the result presented as a smaller graph in figure 2.10. Another reason for this increase in the background could be the presence of amorphous parts in the sample. The data of the annealed thin film Pb_2CrO_5-3, presented in figure 2.11, reveals one large peak (310), which is the same main peak found for a thin film made in the following conditions: T_s= 100 °C, T_a= 450 °C, and t_a= 1.5 h, using an Electron-Beam Evaporation technique [10]. In this case we observe less peaks and the increase in the background is not observed possibly due to the improved crystallization of the thin film which does not allow the x rays to penetrate as deep as in the case of the unannealed thin film. In conclusion, annealing of the thin film enhances the crystallization of a thin film in a preferred direction.

Ceramic sample

The crystal structure of the Pb_2CrO_5, $Pb_{1.95}K_{0.05}CrO_5$, $Pb_{1.875}K_{0.125}CrO_5$, and $Pb_{1.85}La_{0.15}CrO_5$ samples has also been investigated by using the X-ray Diffraction technique. The (hkl)

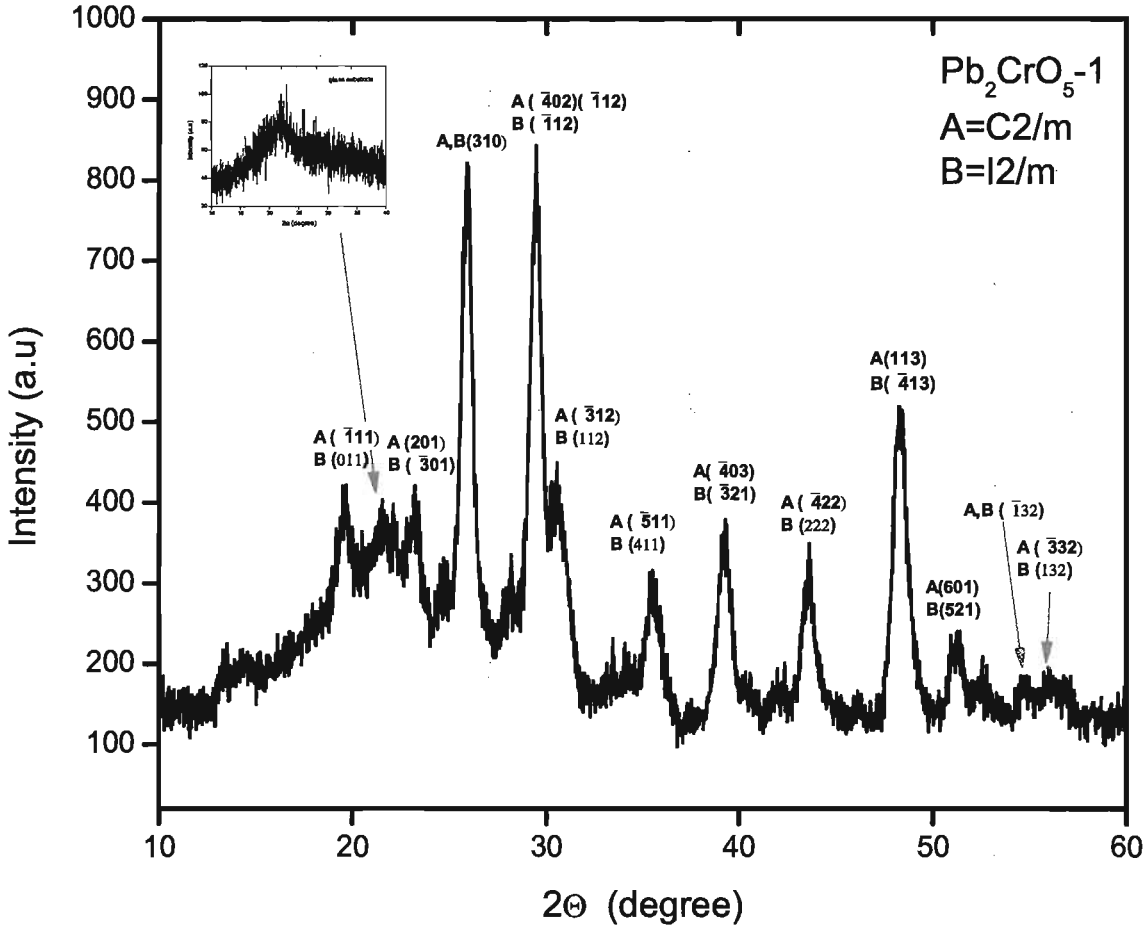

Figure 2.10: **X-ray diffraction data of Pb_2CrO_5-1 thin film**

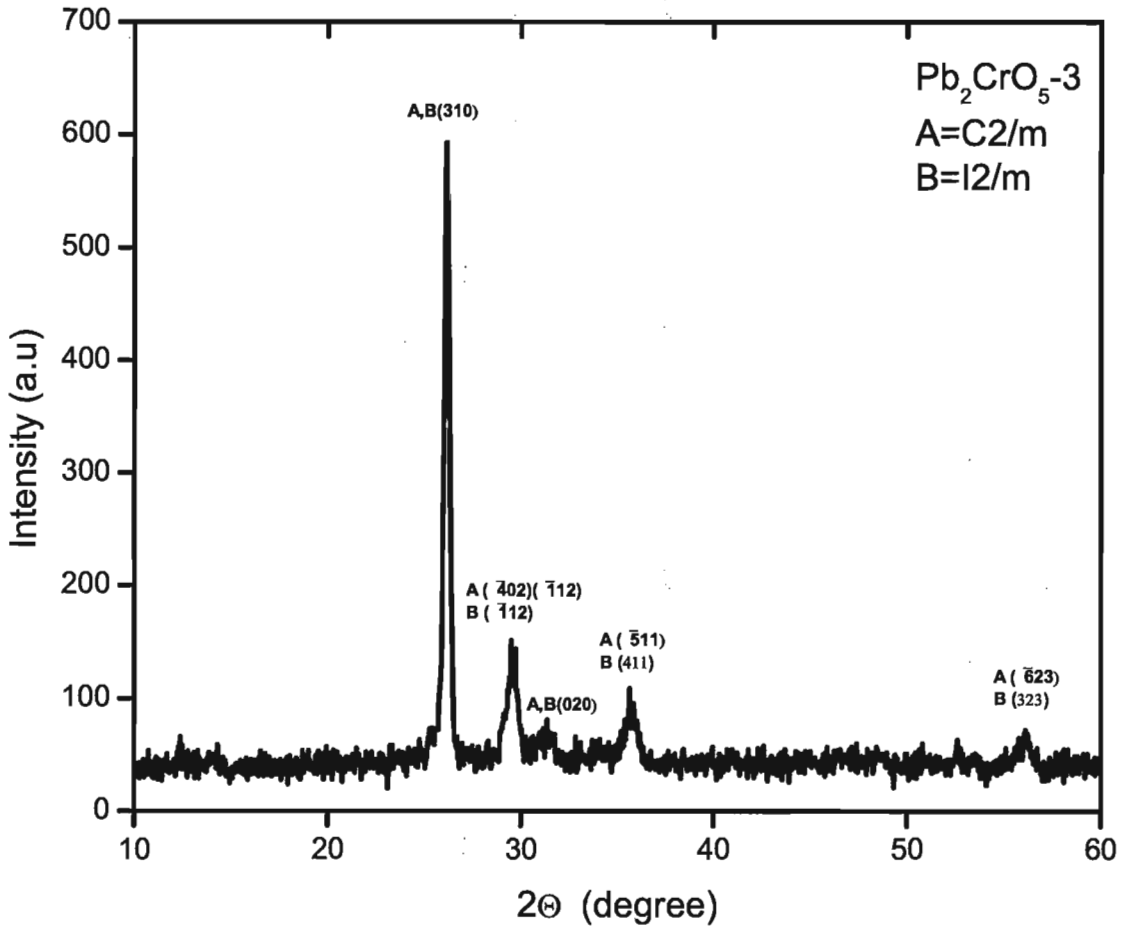

Figure 2.11: **X-ray diffraction data of Pb_2CrO_5-3 thin film**

reflections are compared to the PDF card of the Pb_2CrO_5 compound. The crystal structure of this compound is Monoclinic, but it can have different space groups: C2/m (single face centered) or I2/m (body centered) [15, 20]. In figure 2.12 a result for the X ray diffraction of the Pb_2CrO_5 ceramic sample is given. The strong intensity peaks (310), $(\bar{4}02)$ and $(\bar{1}12)$ are present but also some of the high 2θ angles have strong intensity which was not observed when the X ray powder diffraction was done (see figure 2.13). The reason for this could be a problem of the sample texture. When the X ray diffraction was done on the ceramic sample for fixed 2θ we have observed many peaks while in the case when we used powder of the same compound the data did not have any peaks, as seen from figure 2.14. The values for the 2θ angles found in Pb_2CrO_5 ceramic sample are compared with the angles for these two space groups and presented in Appendix A. All of the 2θ angles found in the Pb_2CrO_5 ceramic sample are found in both structures (C2/m and I2/m) and since the intensities have been normalized it is difficult to determine the percentage of either structure in the sample.

In figure 2.15, the X ray diffraction data for the $Pb_{1.95}K_{0.05}CrO_5$ sample is presented. This experiment was also done using the powder diffraction technique and all of the reflections are found in the Pb_2CrO_5 structure [15] .

From the X ray diffraction pattern for the $Pb_{1.875}K_{0.125}CrO_5$ sample we detect three peaks that are not found in the Pb_2CrO_5 crystal structure (see figure 2.16). This indicates the presence of an impurity phase. A preliminary study has been done as an attempt to determine these impurities. It was found that the impurity phase is likely $Pb_5O_4(CrO_4)$. The results for the three impurity peaks are presented and compared to the peaks of the possible impurity phase from a reference in table 2.2. In table 2.3 we are comparing the first five peaks of the $Pb_5O_4(CrO_4)$ crystal structure with these of our sample of $Pb_{1.875}K_{0.125}CrO_5$ crystal structure. The comparison in

$Pb_{1.875}K_{0.125}CrO_5$	$Pb_5O_4(CrO_4)$[22]
2θ (°)	2θ (°)
20.56	20.75
28.74	28.85
33.10	33.40

Table 2.2: Impurities in $Pb_{1.875}K_{0.125}CrO_5$ sample

Peak	$Pb_5O_4(CrO_4)$ [22]	$Pb_{1.875}K_{0.125}CrO_5$
	2θ (°)	2θ (°)
1st	27.59	27.58
2nd	33.40	33.10
3rd	28.85	28.74
4th	28.39	28.00
5th	30.86	30.90

Table 2.3: Impurity phase $Pb_5O_4(CrO_4)$ in $Pb_{1.875}K_{0.125}CrO_5$ sample

this table is important because the high intensity peaks of the impurity phase have to be present in the sample. By dividing the intensity of the main peak of the Pb_2CrO_5 phase and the intensity of the highest peak of the impurity phase we can estimate that the presence of the impurity phase is approximately the square root of this ratio, that is 1.6 percent [21].

In the result for the La doped sample, in figure 2.17 we can detect five peaks that are not found in the crystal structure of the parent compound. Therefore, they are considered to be impurity phases formed in the sample. The estimated presence of the impurity phase is approximately 2.8 percent. An attempt to determine these impurities is presented in table 2.4. After comparison of the first five peaks for both

$Pb_{1.85}La_{0.15}CrO_5$	$Cr_{1.01}LaO_x$ [23]	$Pb_5O_4(CrO_4)$[22]
2θ (°)	2θ (°)	2θ (°)
22.86	22.85	x
28.30	x	28.39
28.74	x	28.85
32.58	32.54	x
33.28	x	33.40

Table 2.4: Impurities in $Pb_{1.85}La_{0.15}CrO_5$ sample

Peak	$Cr_{1.01}LaO_x$ [23]	$Pb_{1.85}La_{0.15}CrO_5$
	2θ (°)	2θ (°)
1st	32.54	32.58
2nd	46.71	46.30
3rd	58.07	58.24
4th	22.85	22.84
5th	40.15	39.76

Table 2.5: Impurity phase $Cr_{1.01}LaO_x$ in $Pb_{1.85}La_{0.15}CrO_5$ sample

phases to the peaks from X ray diffraction data of the $Pb_{1.85}La_{0.15}CrO_5$ sample it was likely that the impurities are $Cr_{1.01}LaO_x$ and $Pb_5O_4(CrO_4)$. This is presented in the two tables: for $Cr_{1.01}LaO_x$ in table 2.5 and for $Pb_5O_4(CrO_4)$ in table 2.6.

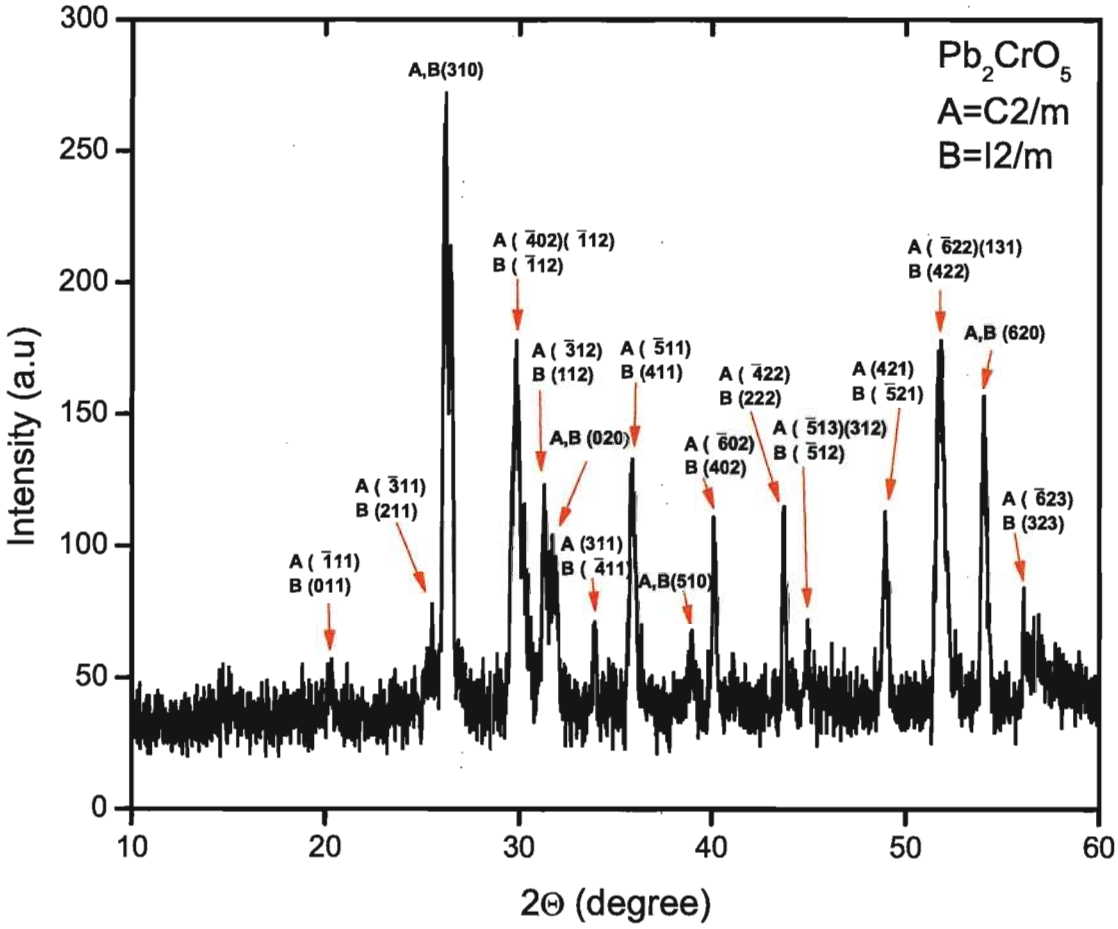

Figure 2.12: **X-ray diffraction data of Pb_2CrO_5 ceramic sample**

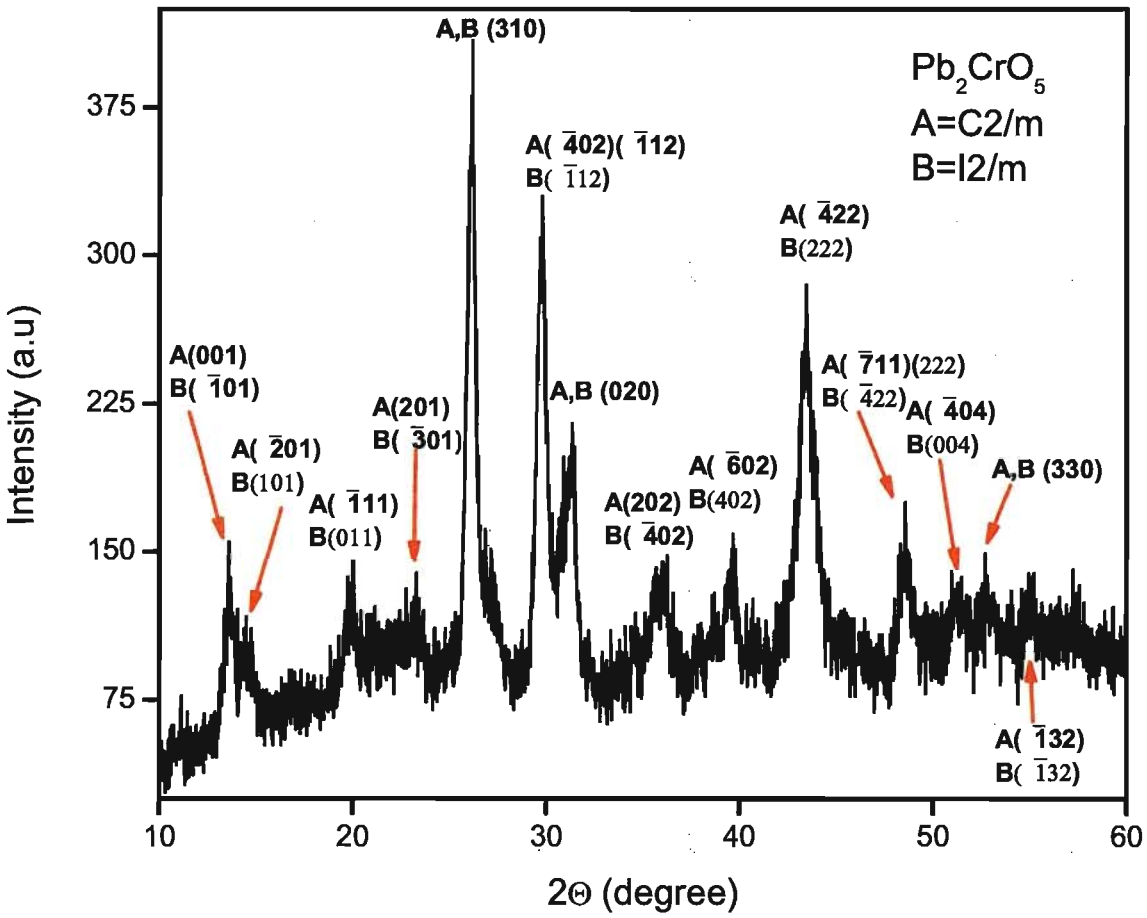

Figure 2.13: **X-ray powder diffraction data of Pb_2CrO_5 sample**

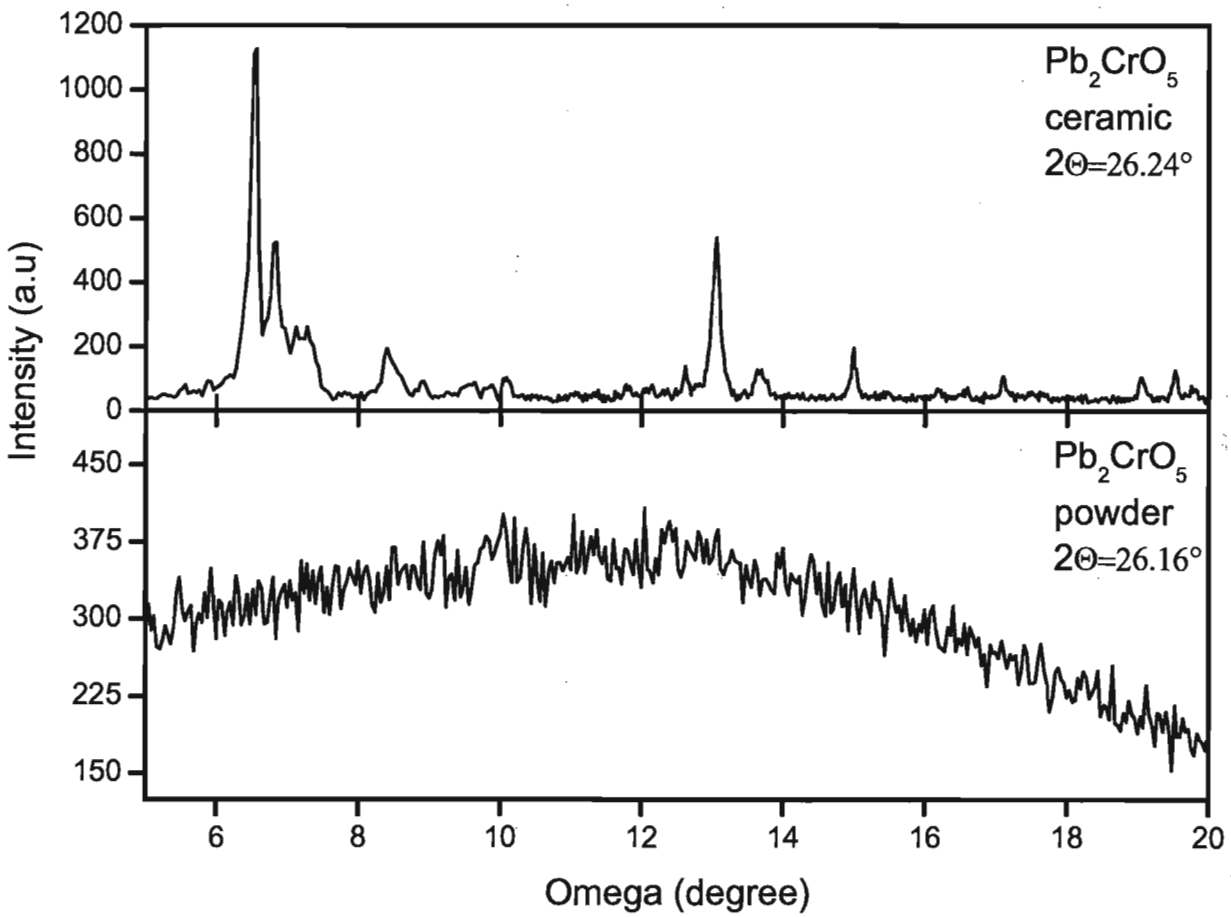

Figure 2.14: **X-ray diffraction of Pb_2CrO_5 ceramic and powder samples**

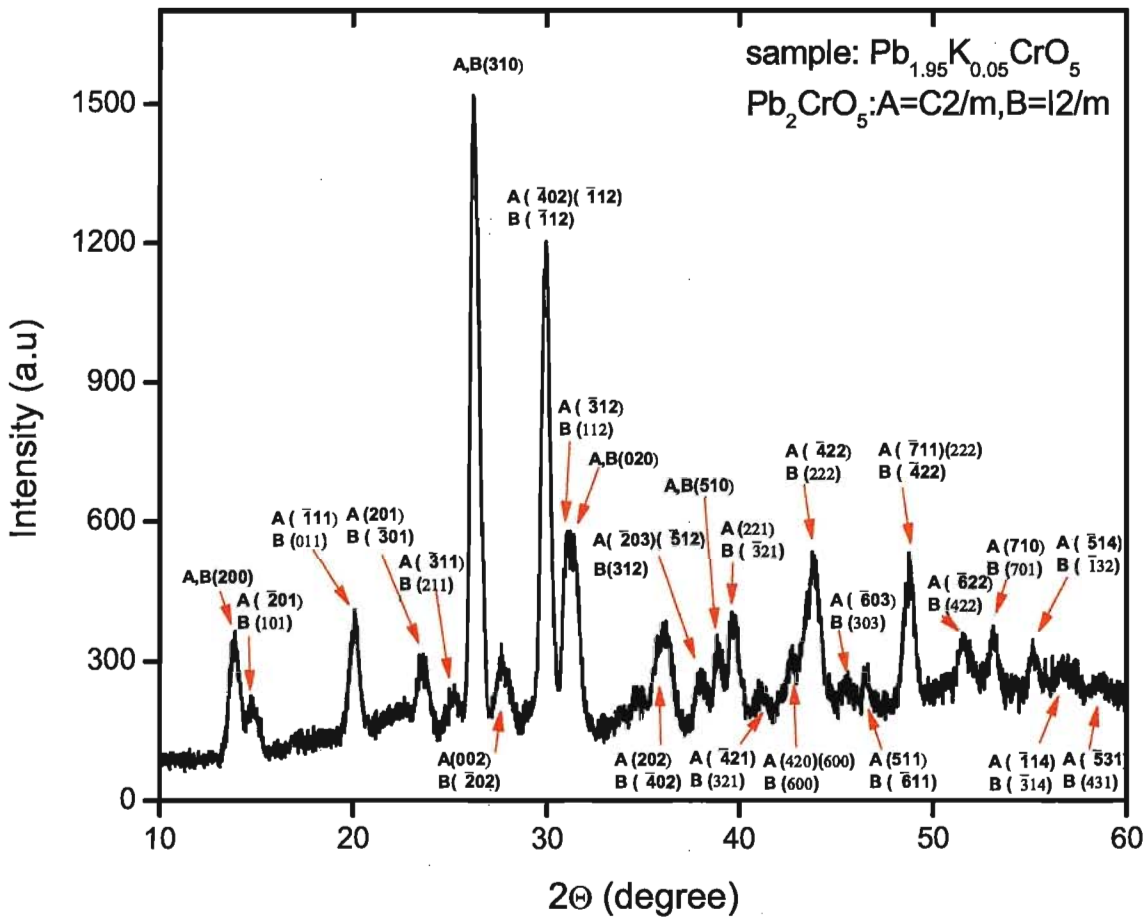

Figure 2.15: **X-ray diffraction data of $Pb_{1.95}K_{0.05}CrO_5$ sample**

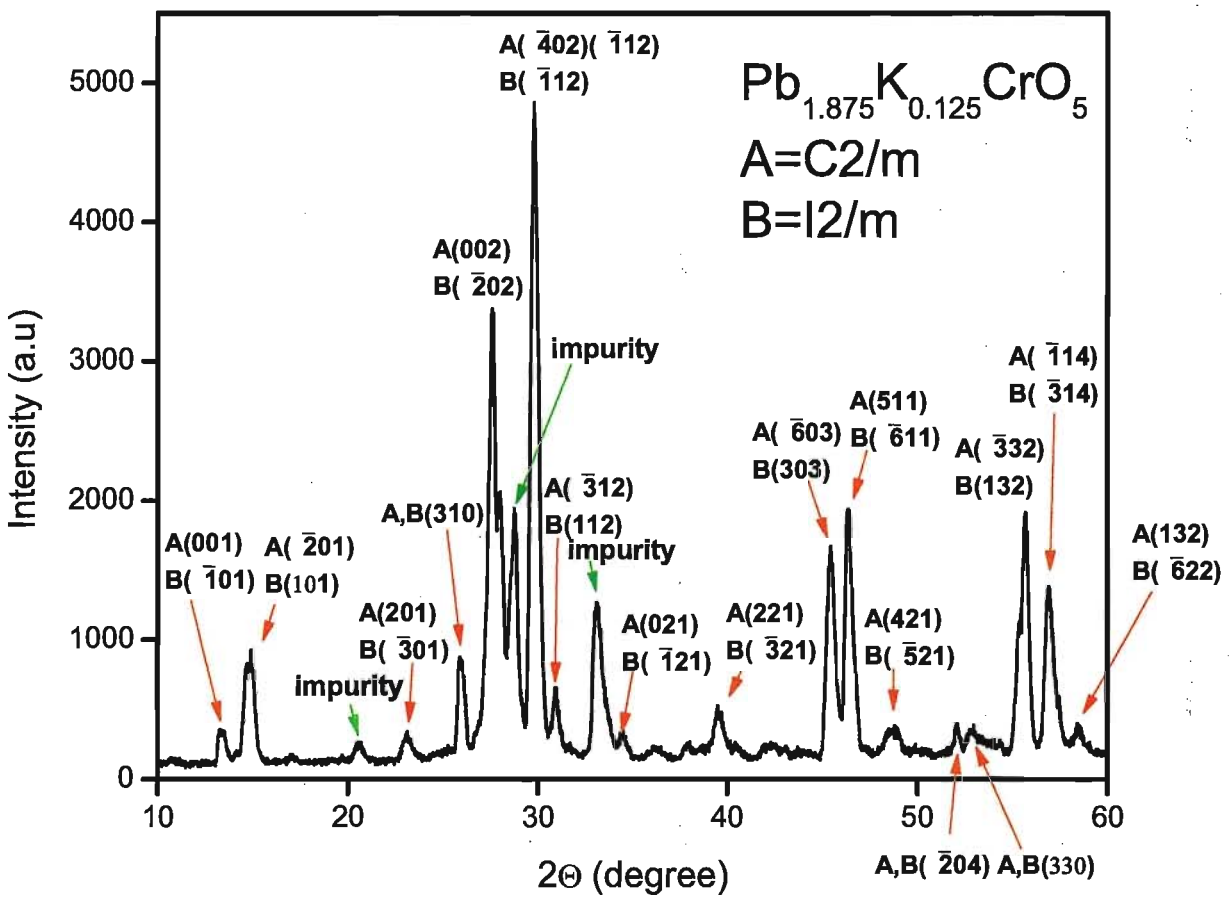

Figure 2.16: **X-ray diffraction data of $Pb_{1.875}K_{0.125}CrO_5$ sample**

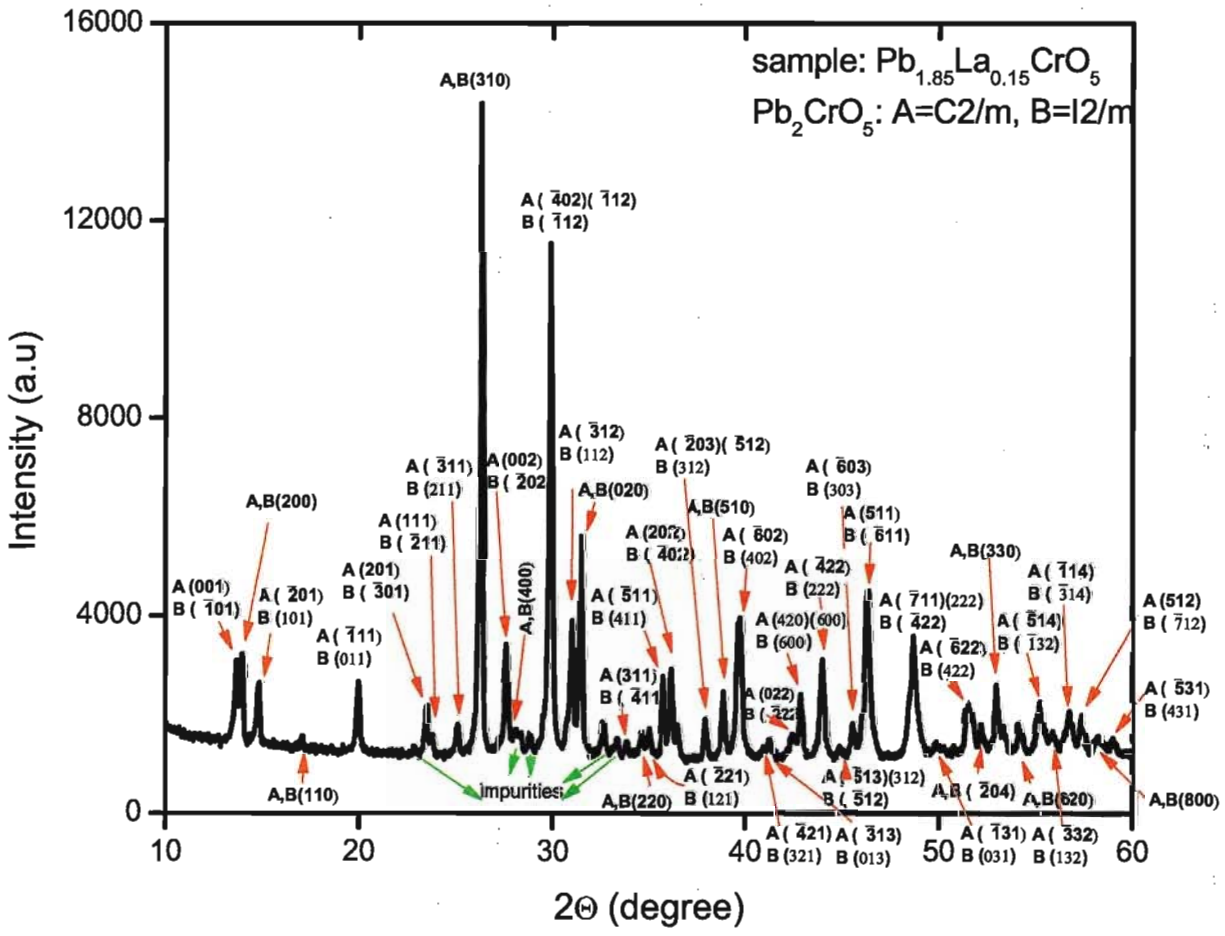

Figure 2.17: **X-ray powder diffraction data of $Pb_{1.85}La_{0.15}CrO_5$ sample**

Peak	$Pb_5O_4(CrO_4)$[22]	$Pb_{1.85}La_{0.15}CrO_5$
	2θ (°)	2θ (°)
1st	27.59	27.58
2nd	33.40	33.28
3rd	28.85	28.74
4th	28.39	28.30
5th	30.86	31.00

Table 2.6: Impurity phase $Pb_5O_4(CrO_4)$ in $Pb_{1.85}La_{0.15}CrO_5$ sample

Chapter 3

Experimental Techniques and Results

3.1 High Temperature Resistance Measurements

3.1.1 Experimental Technique

To measure the resistance of the Pb_2CrO_5 and K or La doped ceramic samples we used an experimental set-up that is shown in figure 3.1. The ceramic sample was placed between two quartz cylinders and suspended by a spring as shown in figure 3.2. Four platinum wires were welded together in small rectangular plates, two wires per plate. The plates were placed between the sample and one of the quartz cylinders. That is how the contacts were made. The schematic diagram is shown in figure 3.3. This system was placed in a quartz tube and then in a furnace. On the one end of the quartz tube there are four openings: two for gas inlet and outlet, one for the four platinum wires and one for the thermocouple that was placed next to the position of the sample. Through two of the platinum wires, one from each plate we applied a constant current, 10 nA, and through the other two wires we measured the voltage. The resistance is then calculated from the measured voltage using Ohms law.

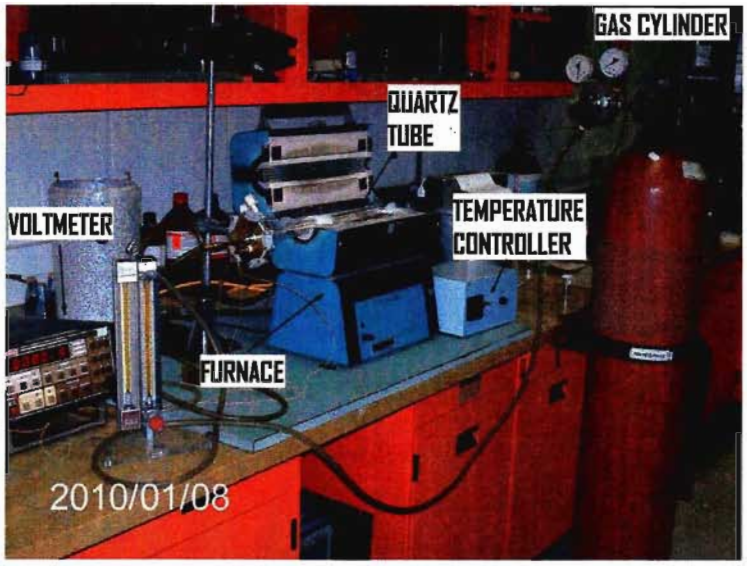

Figure 3.1: **High Temperature Resistivity Measurement, Experimental set-up**

Figure 3.2: **High Temperature Resistivity Measurement, Sample position in the quartz tube**

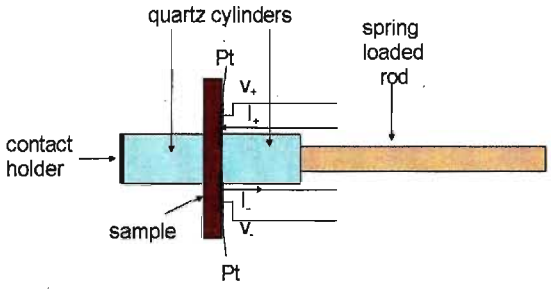

Figure 3.3: **High Temperature Resistivity Measurement, Schematic diagram**

3.1.2 Experimental Results

The high temperature resistivity results are plotted as Resistance vs Temperature graphs. The Pb_2CrO_5 ceramic sample is conducting in air but its resistance increases to high values that are not measurable with our equipment. This increase in resistance is observed in the region between 300 K and 500 K as it can be seen in figure 3.4. The same increase in resistance was observed when cooling down. In figure 3.5 the resistivity for the Pb_2CrO_5 ceramic sample is plotted as a function of the temperature and also in the small graph the data for high temperatures, above 900 K is shown. From figure 3.6 we have calculated the energy gap of the sample and the gap is found to be 1.97 eV which is less than the energy gap determined from optical absorption experiments, 2.3-2.4 eV (see section 1). The conductivity in the intrinsic region in a semiconductor is dominated by the exponential dependence of the temperature and from this relationship we can calculate the energy gap of the sample as shown with

equations 3.1,3.2, and 3.3.

$$R \sim e^{\frac{E_g}{2 \cdot k_b \cdot T}} \tag{3.1}$$

$$ln(R) = ln(A) + \frac{E_g}{2 \cdot k_b \cdot T} \tag{3.2}$$

$$E_g = 2 \cdot k_b \cdot m \tag{3.3}$$

In these equations A is a constant of proportionality, k_b is the Boltzman constant and m is the slope from graph where ln(R) is plotted versus 1/T [24].

The resistance of the Pb_2CrO_5 ceramic sample in Argon or Oxygen gas was measured and as we can see from figure 3.7 the temperature at which the measuring of the resistance of the sample begins, shifts to a higher value. High temperature resistivity measurements were also carried out on the $Pb_{1.95}K_{0.05}CrO_5$ and $Pb_{1.85}La_{0.15}CrO_5$ ceramic samples and as we can see from figure 3.8 the doping of the sample with K and La atoms decreases the resistance. The energy gap for the $Pb_{1.95}K_{0.05}CrO_5$ sample is calculated from figure 3.9 to be 1.21 eV.

3.2 Magnetism

3.2.1 SQUID Magnetometer

There are three sources of magnetism in free atoms: the spin of an electron, the orbital momentum, and the change in the orbital momentum of an electron. The electron is spinning and by that can be considered as an electric current loop. The magnetic moment produced by this current contributes to the total magnetization of the material. The electron is also orbiting around the nucleus and this is another contribution to the total magnetization of the material. Finally, if a material is placed in a magnetic field the magnetic field will affect the orbital momentum. The first two, the spin and the orbital contribution are paramagnetic contributions while the change in orbital

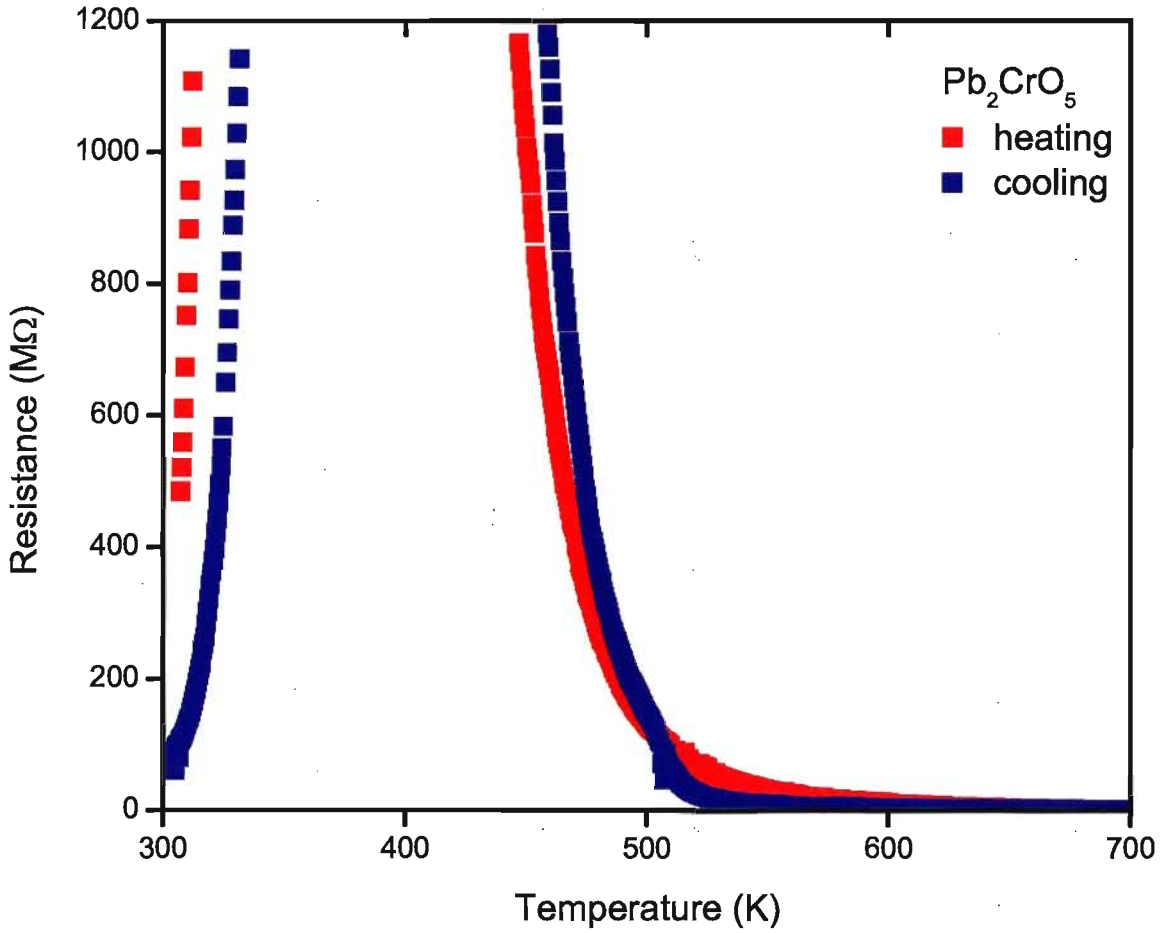

Figure 3.4: **High Temperature resistance of Pb_2CrO_5 ceramic sample in air**

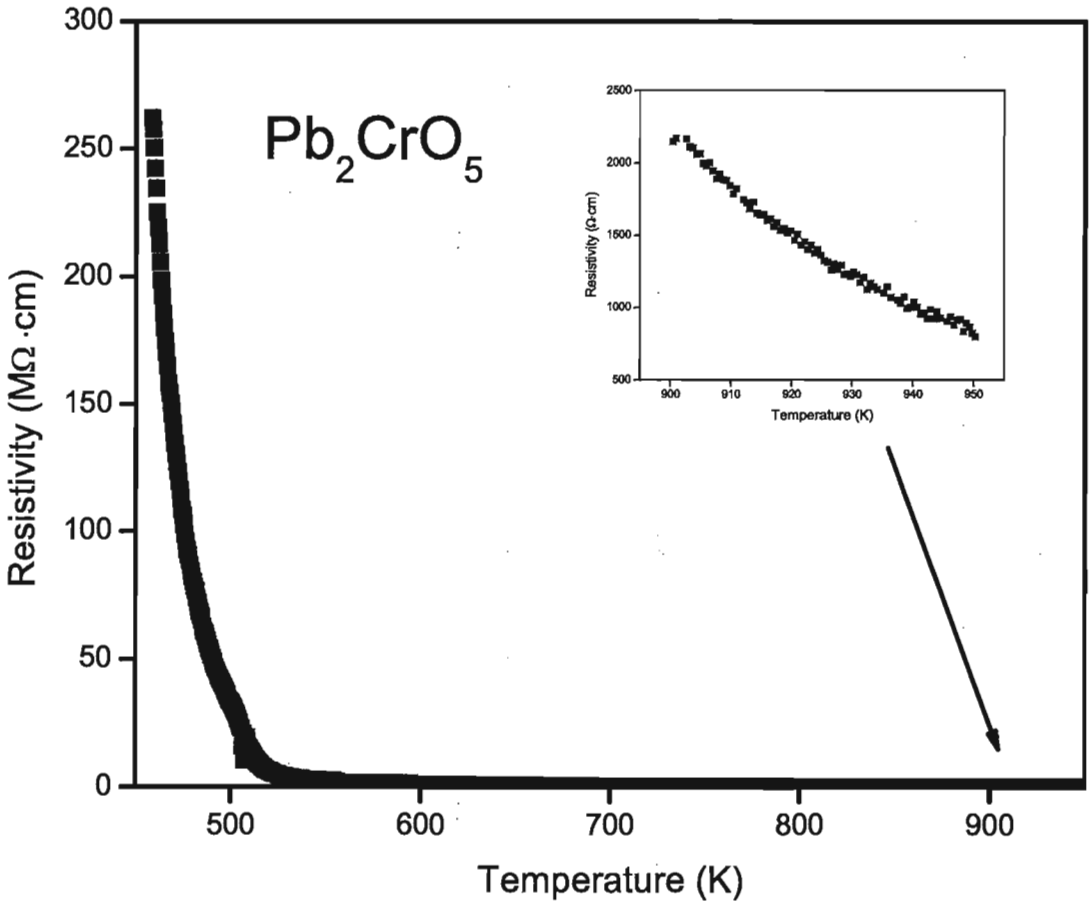

Figure 3.5: **High Temperature resistivity of Pb_2CrO_5 ceramic sample**

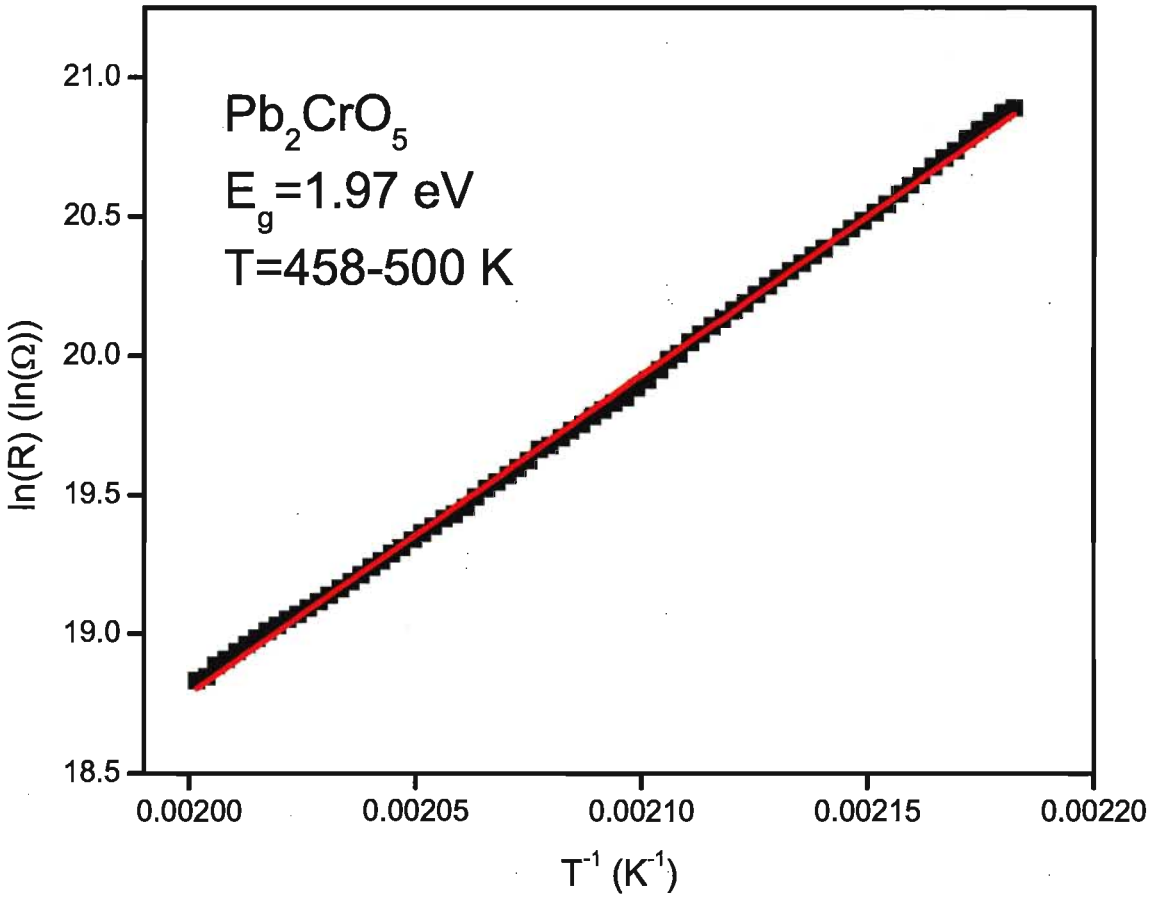

Figure 3.6: **Energy gap of Pb_2CrO_5 ceramic sample**

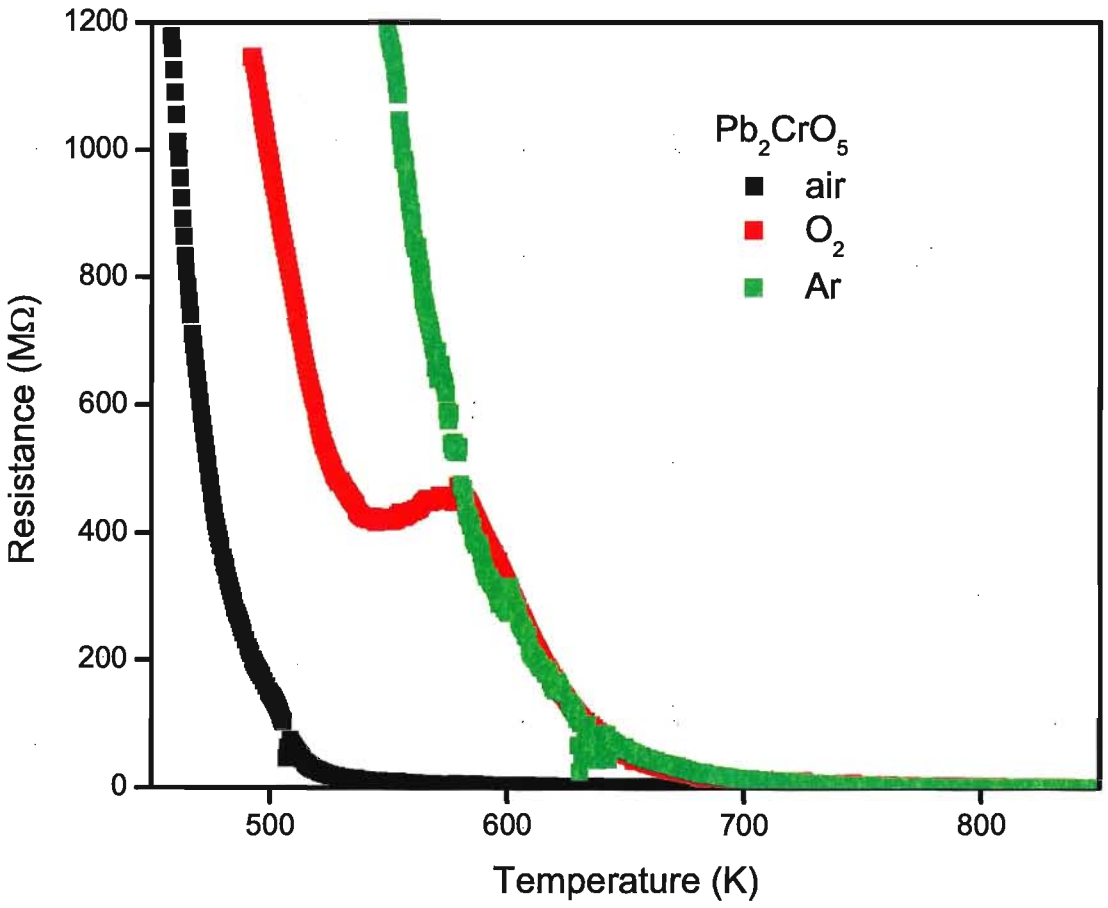

Figure 3.7: **Resistance of Pb_2CrO_5 ceramic sample in different gas environments**

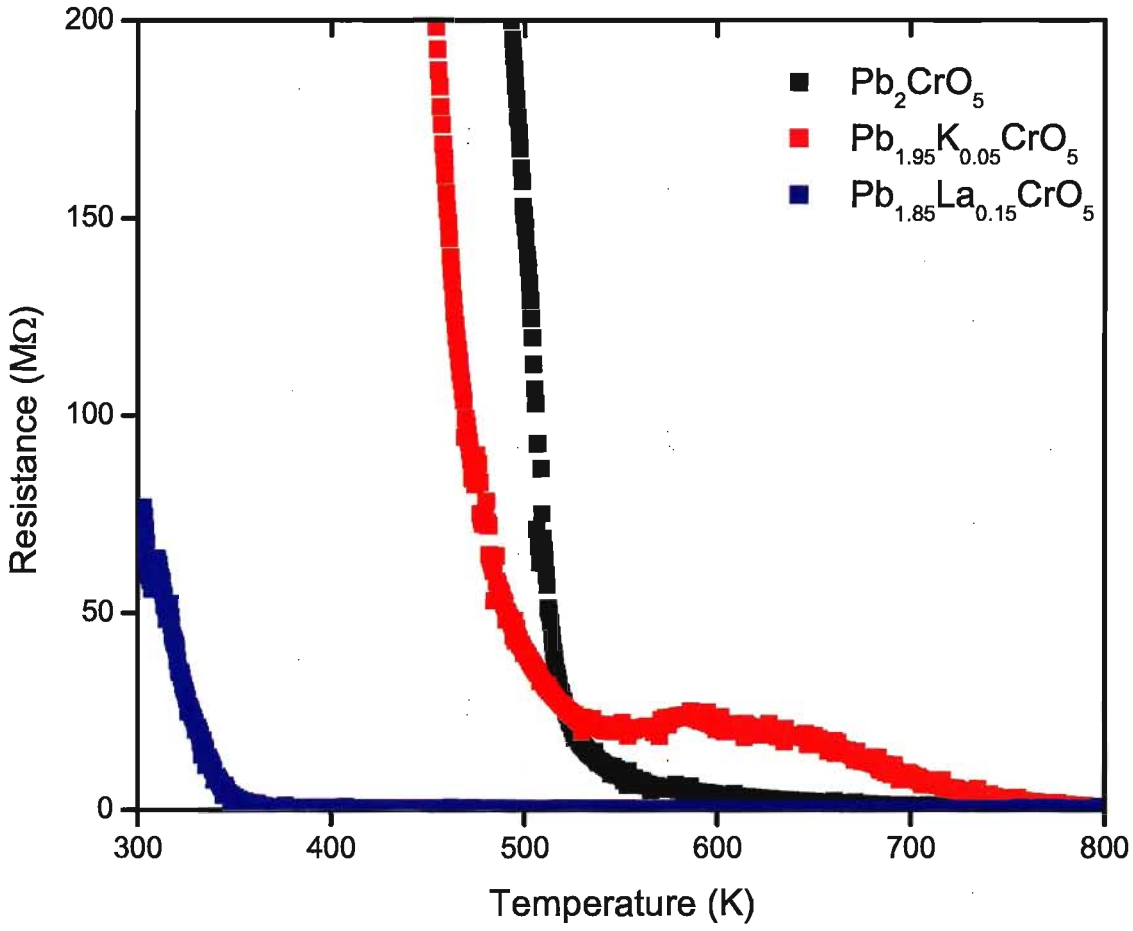

Figure 3.8: **High Temperature Resistance of Pb_2CrO_5, $Pb_{1.95}K_{0.05}CrO_5$, and $Pb_{1.85}La_{0.15}CrO_5$ in air**

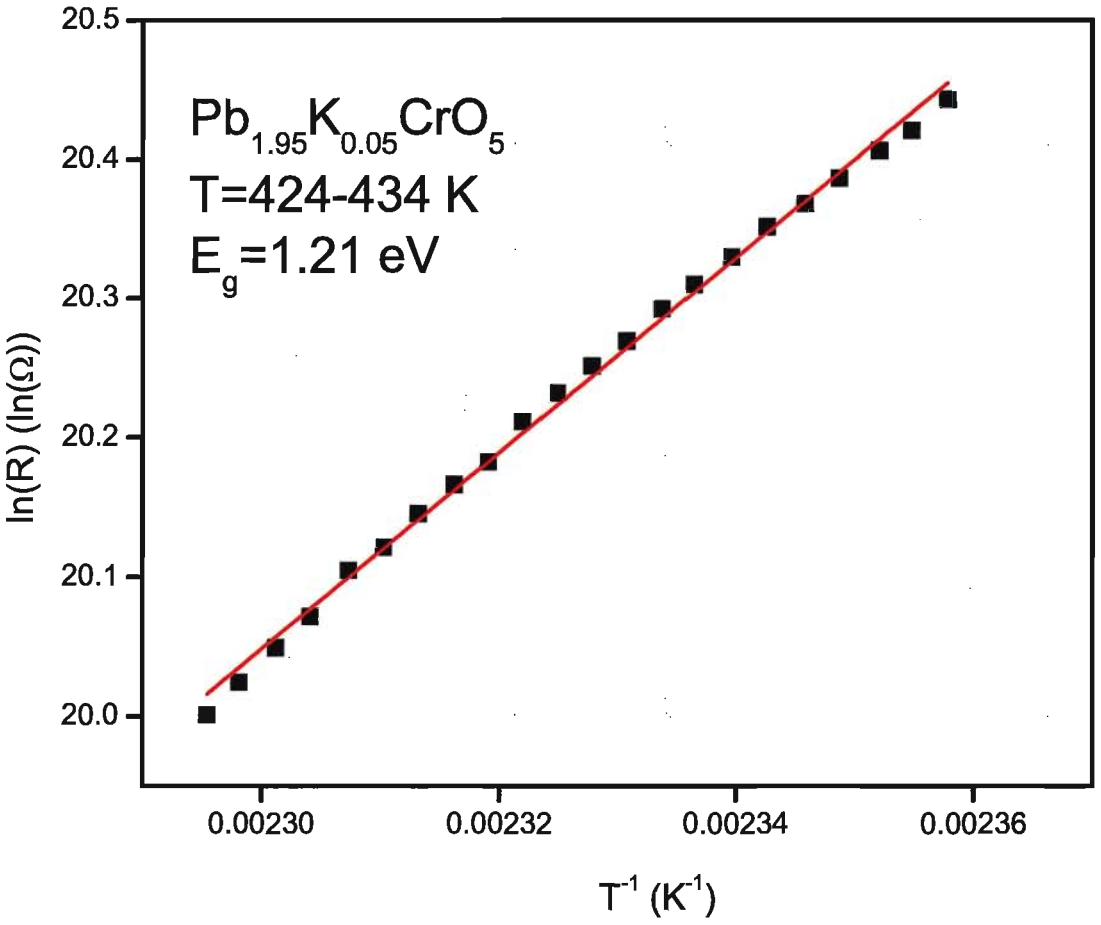

Figure 3.9: **Energy gap of $Pb_{1.95}K_{0.05}CrO_5$**

momentum provides a diamagnetic contribution to the total magnetization of the material. The magnetization is defined as a magnetic moment per unit volume. If we divide the magnetization with the magnitude of the applied magnetic field we can calculate the magnetic susceptibility of the material. Materials with positive magnetic susceptibility are paramagnetic and the net magnetization is in the same direction as the applied magnetic field. Materials with negative susceptibility are called diamagnetic and in this case the net magnetization is opposing the applied magnetic field. Ferromagnetism occurs in materials that have a spontaneous magnetic moment when there is no magnetic field applied or in a case when after a magnetic field has been applied and removed, the material is still magnetized. The temperature above which a material loses its spontaneous magnetization and becomes paramagnetic is called the Curie temperature. Antiferromagnetism occurs in materials that have spins in an antiparallel arrangement in such a way that the net moment is zero. The temperature above which a material loses this magnetization and becomes paramagnetic is called the Neél temperature[25].

To determine the magnetic properties of the samples in this research we have measured the magnetic moment as a function of temperature using a SQUID magnetometer. SQUID is an abbreviation for Superconducting QUantum Interference Device. The samples were pieces of ceramic disks of irregular shape ($\sim$ rectangular) and their mass was measured. The mass was included in the determination of the total magnetization of the sample by dividing the magnetic moment with the mass. This result yields the magnetic moment per gram. Samples were mounted on a straw; a clear straw was used because it has a small magnetic susceptibility. The sample is secured by making two small cuts in the straw forming a strip that is pushed inside which the sample can be threaded through. Also a small piece of tape can be added on the bottom part of the straw to avoid an accidental fall of the sample into the

sample chamber. The straw is mounted on the rod using tape. The sample is placed inside the airlock space at 300 K. After closing the airlock space is purged (1 to 3 times) in order to avoid oxygen presence. The next step is to place the sample in the sample chamber where the magnetic moment is measured. This is done when the temperature in the sample chamber is 300 K and once the sample is inside we purge the system again. The sample chamber was then cooled down to 5 K at a rate of 10K/min. After a magnetic field is applied to the sample, the sample is centered in such a way that its position is at the halfway mark of the scan length. The sample is moved through the pick-up coils that detect the voltage. The MPMS MultiVu records this voltage as a function of sample position, and this is recorded as raw data. This data is then used to compute the magnetic moment using a measurement algorithm [26].

3.2.2 Experimental Results

Pb_2CrO_5 ceramic sample is paramagnetic and as it can be seen from figure 3.10 there is a decrease of the magnetic moment at temperatures above 300 K. This transition begins at 283 K. The inverse of susceptibility as a function of temperature is plotted in figure 3.11. From this graph we can determine that temperature T_1, the transition temperature, is at $\sim$ 310 K. As the temperature is approaching zero Kelvin, the susceptibility is also approaching zero. The $Pb_{1.85}$ $La_{0.15}CrO_5$ ceramic sample is also paramagnetic. The magnetic moment is greater than the one measured in the Pb_2CrO_5 sample. This can be a result of the unpaired electrons from the Cr^{3+} ($3d^3$) ions, as described in section 2.1. In the result shown in figure 3.12 we can note the transition begins at 287 K. When the inverse of the susceptibility is plotted (see figure 3.13) as a function of temperature, the transition temperature is found to be $\sim$ 295 K. The paramagnetism in these samples could be a result of impurities

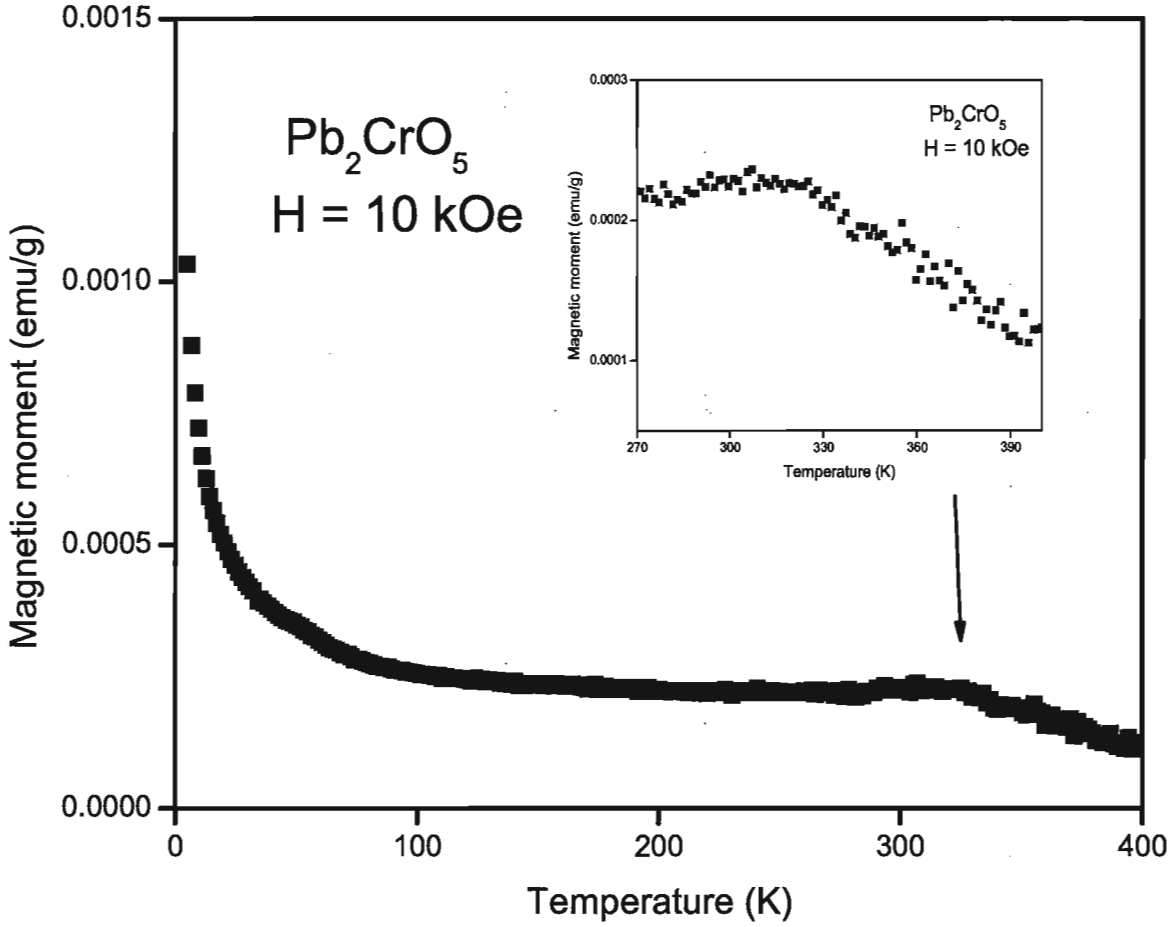

Figure 3.10: **Magnetization of Pb_2CrO_5 ceramic sample**

caused by the stochiometric deficiency of one of the elements in the compound. For example, oxygen deficiency will cause the valence of chromium atoms to change and as a result the Cr^{3+} ($3d^3$), Cr^{2+} ($3d^4$) ions will be present in the structure. The unpaired electrons of the Cr^{3+} ion could be the cause of the paramagnetism in these samples. When the magnetization measurement is done on the K doped sample, the transition observed in the parent sample and the La doped sample is not observed as seen from figure 3.14. The transition in K doped samples is from a paramagnetic to diamagnetic state. The temperature at which this transition occurs is $T_1 \sim 50$ K for $Pb_{1.95}K_{0.05}CrO_5$ and $T_2 \sim 250$ K for $Pb_{1.875}K_{0.125}$ CrO_5. The paramagnetism and the transition temperature increase with the increase in the number of K atoms in the structure. Since diamagnetism was not observed in Pb_2CrO_5 we can conclude that the diamagnetic contribution is a result of the presence of the K atoms in the structure. The inverse susceptibility as a function of temperature below the transition temperature for the $Pb_{1.875}K_{0.125}$ CrO_5 sample is shown in figure 3.15. Using the slope from the graph the effective moment can be calculated in units of Bohr magnetons. The equation used for this calculation is 3.4 where C_m is equal to the inverse of the slope [27]. The sample is paramagnetic as the temperature approaches zero. The reciprocal susceptibility also approaches zero.

$$p_{eff} = 2.82 \cdot \sqrt{C_m} \tag{3.4}$$

The magnetization measurement of the thin film Pb_2CrO_5-1 is presented in figure 3.16 and we can note that the sample is weakly paramagnetic and becomes diamagnetic at high temperature. The diamagnetism could be a result from the glass substrate. In figure 3.17 the mass magnetization as a function of the applied magnetic field is presented for the Pb_2CrO_5 ceramic sample and compared to the result of the K doped samples. As we can see from the graph the doping of the samples causes increase in

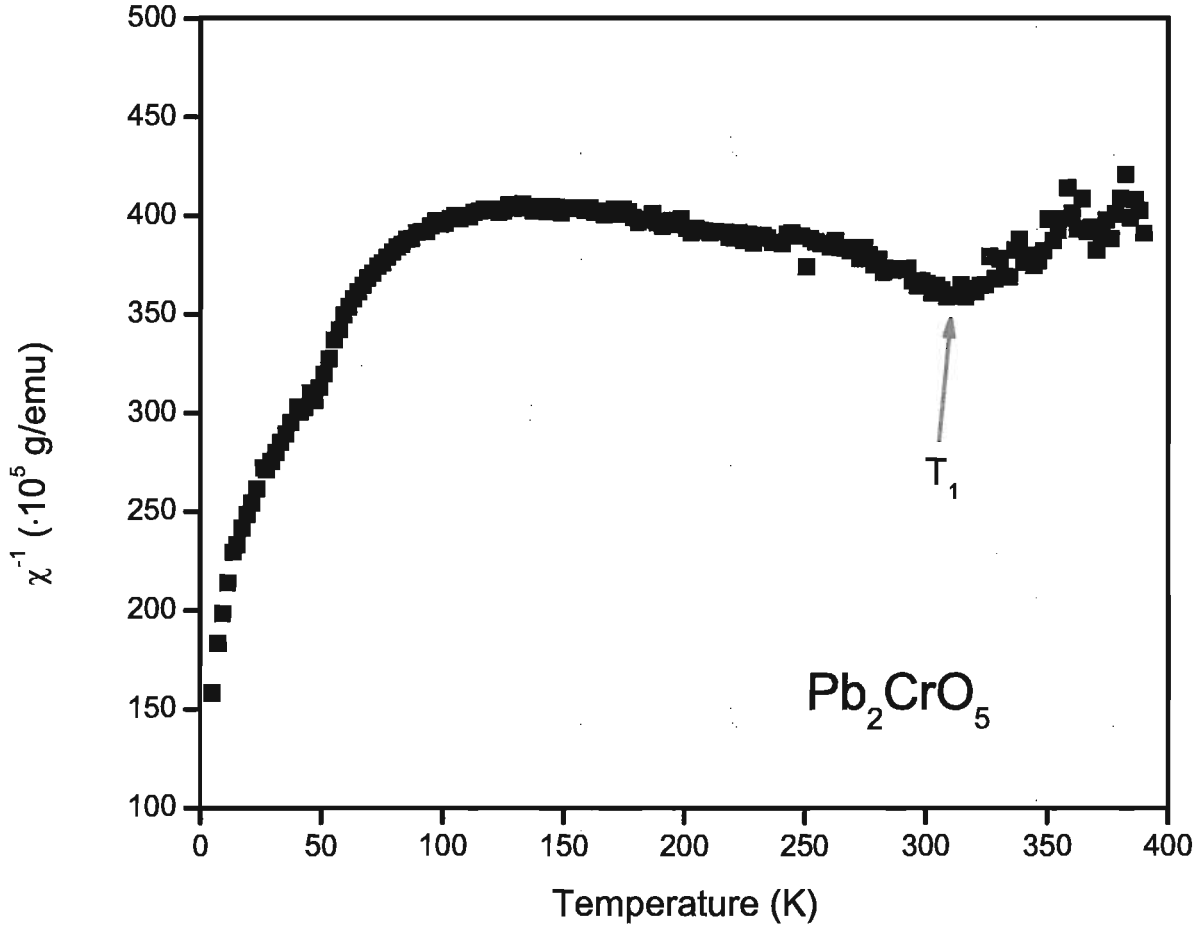

Figure 3.11: **Inverse susceptibility as a function of temperature of Pb_2CrO_5 ceramic sample**

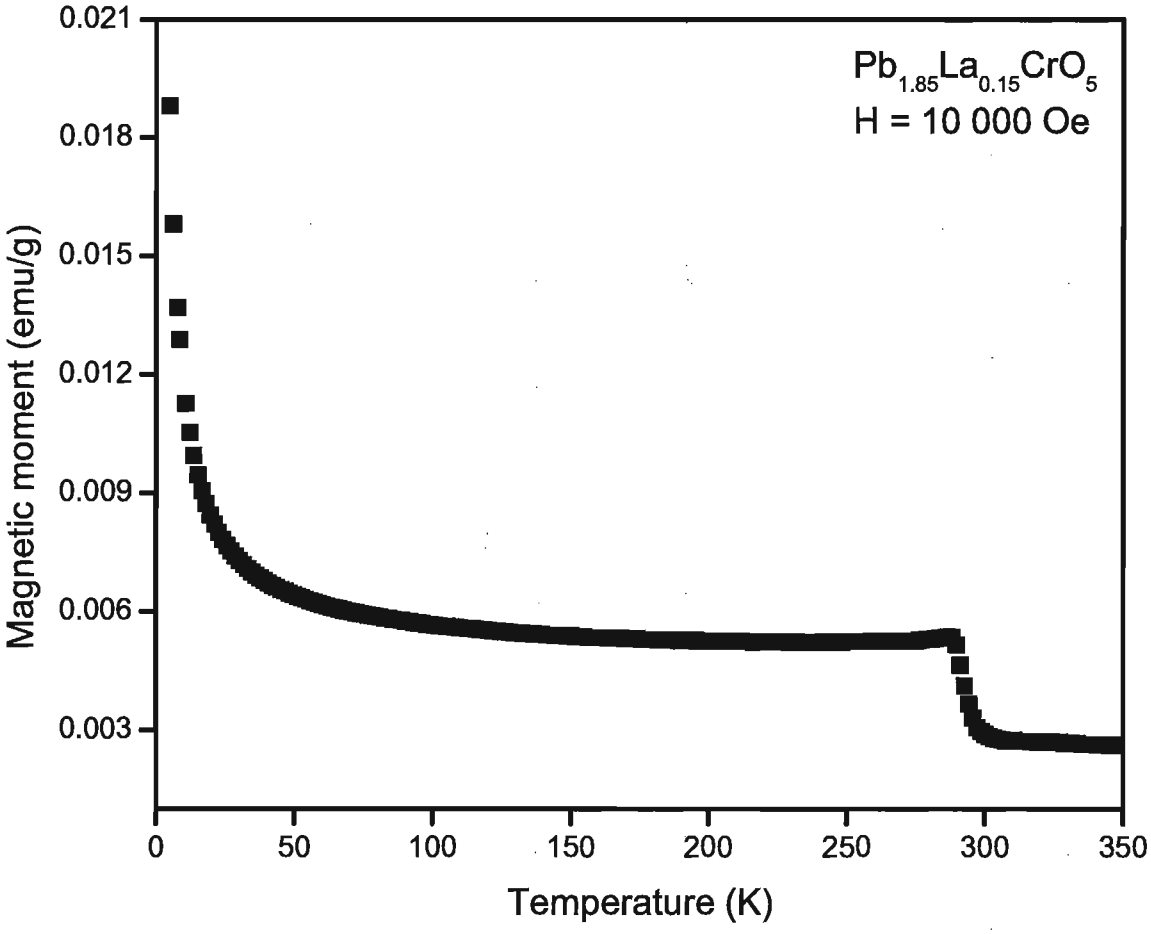

Figure 3.12: **Magnetization of $Pb_{1.85}$ $La_{0.15}CrO_5$ ceramic sample**

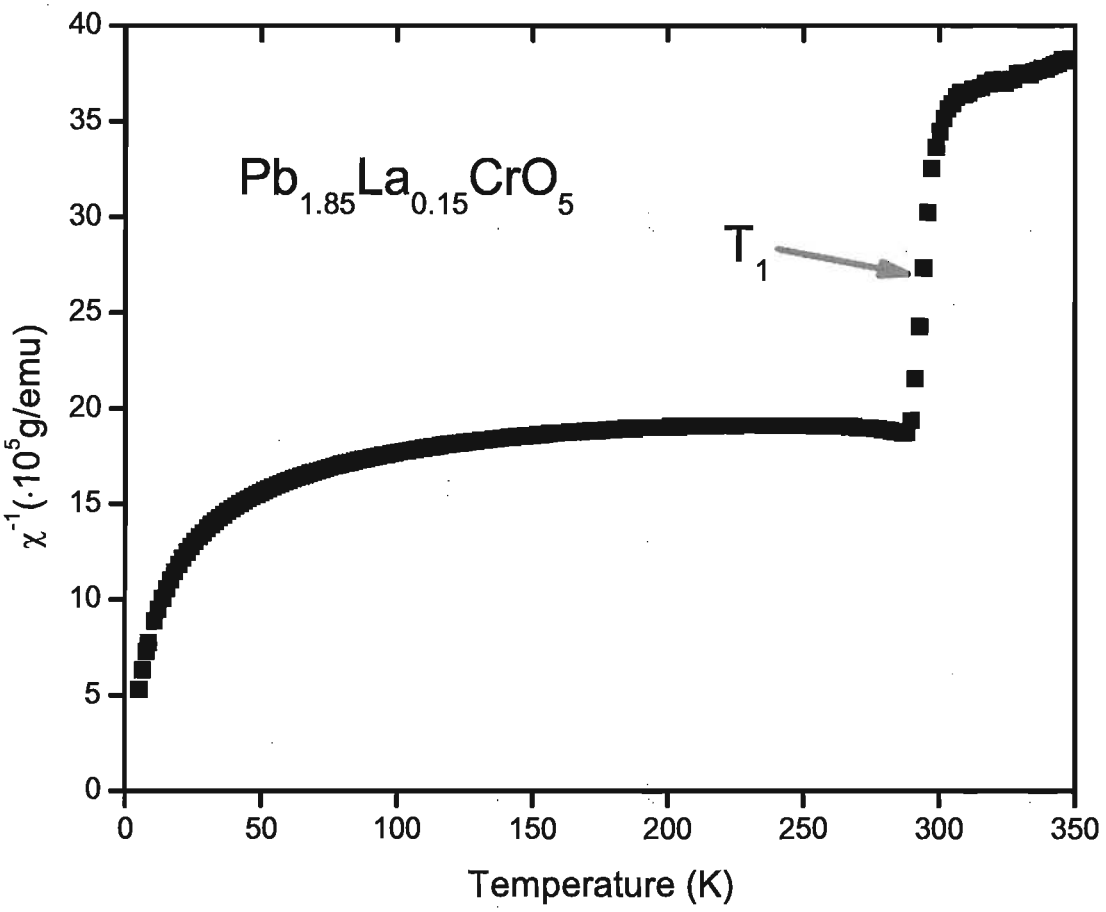

Figure 3.13: **Inverse susceptibility as a function of temperature of $Pb_{1.85}La_{0.15}CrO_5$ ceramic sample**

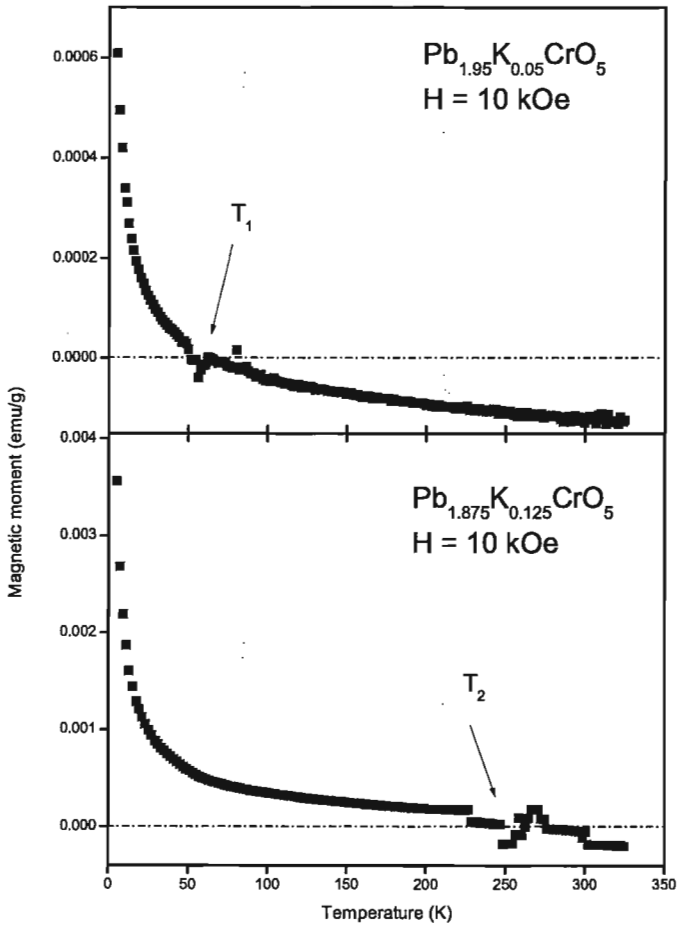

Figure 3.14: **Magnetization of $Pb_{1.95}K_{0.05}CrO_5$ and $Pb_{1.875}K_{0.125}$ CrO_5 ceramic samples**

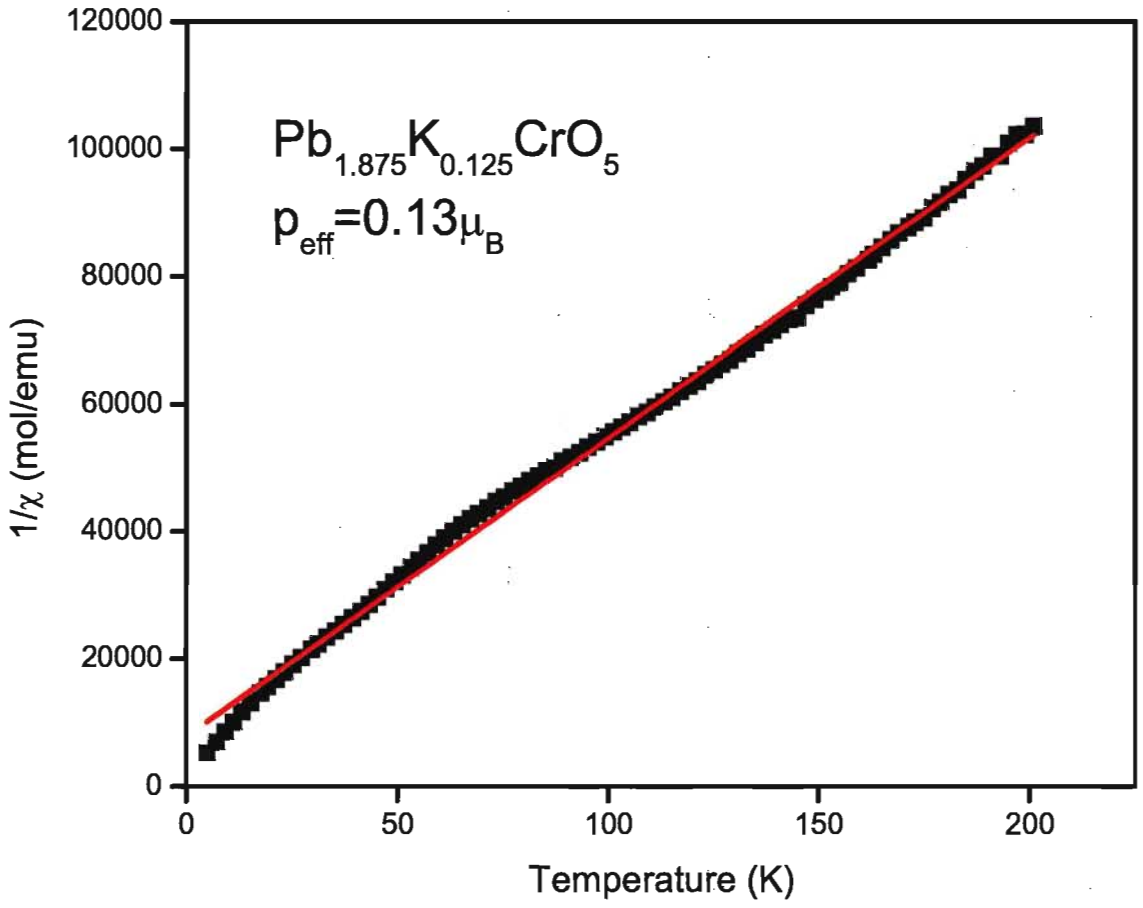

Figure 3.15: **Inverse susceptibility as a function of temperature of $Pb_{1.875}K_{0.125}$ CrO_5 ceramic sample**

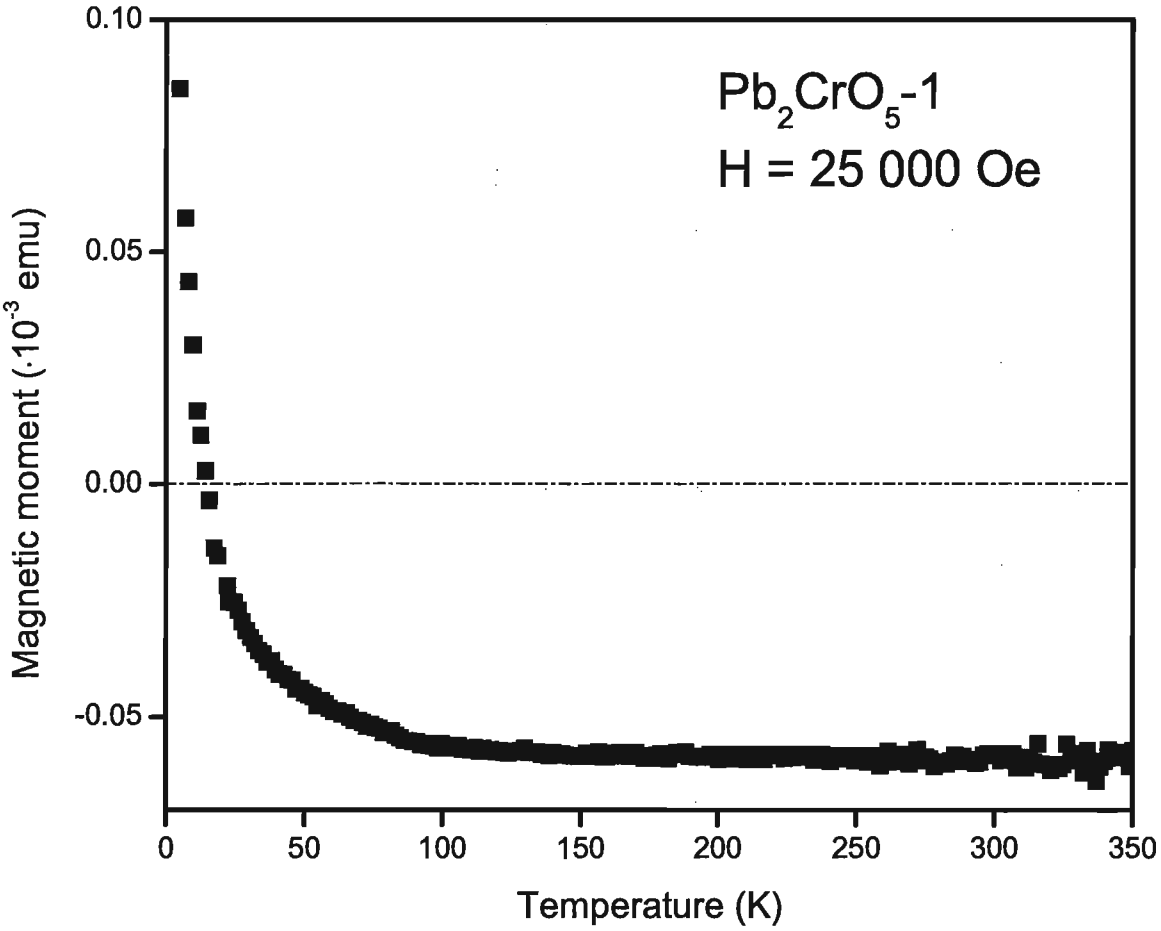

Figure 3.16: **Magnetization of Pb_2CrO_5-1 thin film**

the magnetic moment and also we observe saturation. The same measurement was done on the La doped sample and from the result we can see that saturation is not observed.

3.3 Differential Scanning Calorimetry

3.3.1 DSC Technique

DSC is an abbreviation for Differential Scanning Calorimetry, an important technique that registers changes in heat capacity of different materials. This method can be used to determine melting, crystallization, glass transitions and other effects (see figure 3.19). The Differential Scanning Calorimeter contains a heater with two positions, one for the sample that is being investigated and the other for the reference. Usually an empty capsule is used as a reference in the measurements. The sample and the reference sample are both under the same heat flow. If the sample undergoes a transition, the heat flow will be disturbed and the system has to adjust for this change to maintain the sample and the reference at the same temperature. In this process some transitions require more energy and some release energy. An endothermic peak is observed when energy is being absorbed; an exothermic peak when energy is being released. Usually the measurement is done by heating and cooling at constant change in degrees over time. Air is blowing constantly over the sample and reference and this can be used for measurements in different gas environments [28].

3.3.2 Experimental Results

For the Pb_2CrO_5 and K or La doped ceramic samples we used Aluminum capsules, and as a reference we used an empty Aluminum capsule. The experiment was conducted

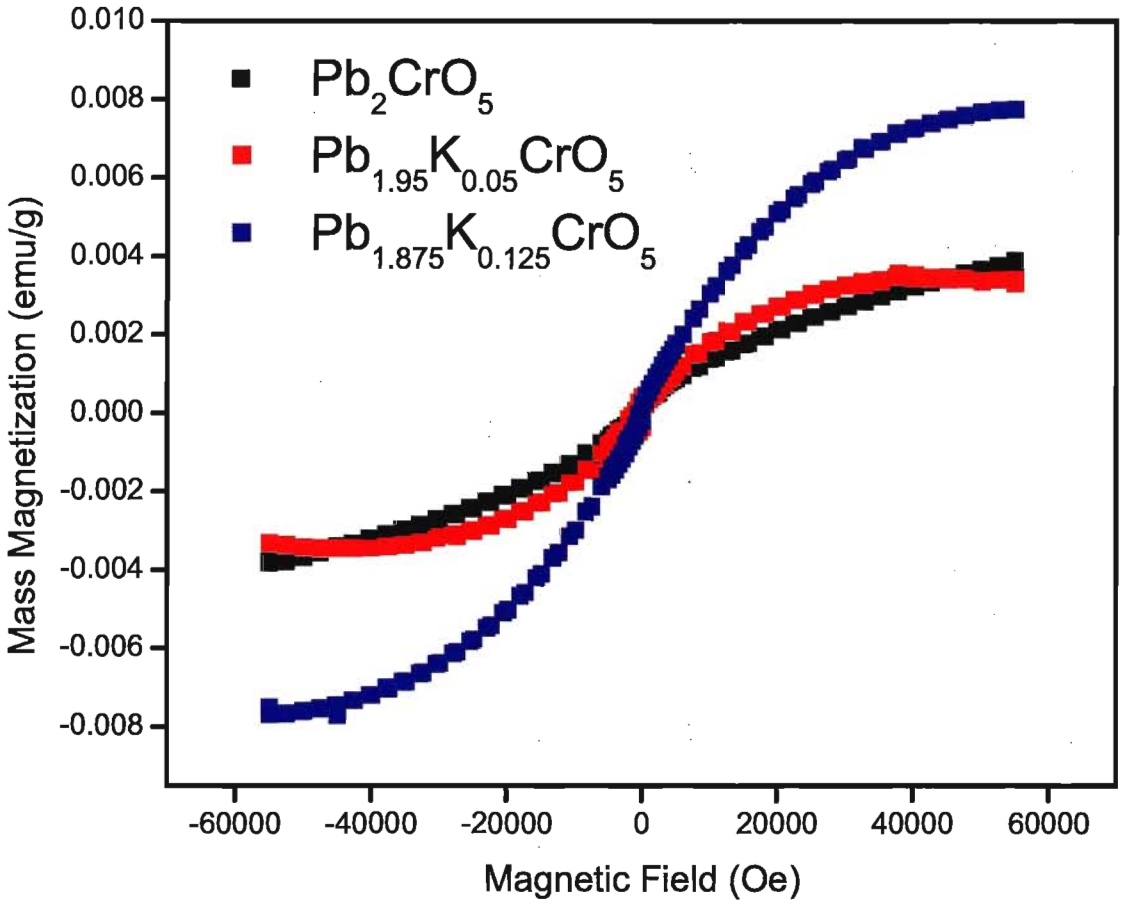

Figure 3.17: **Mass magnetization as a function of the applied magnetic field of Pb_2CrO_5 ceramic sample**

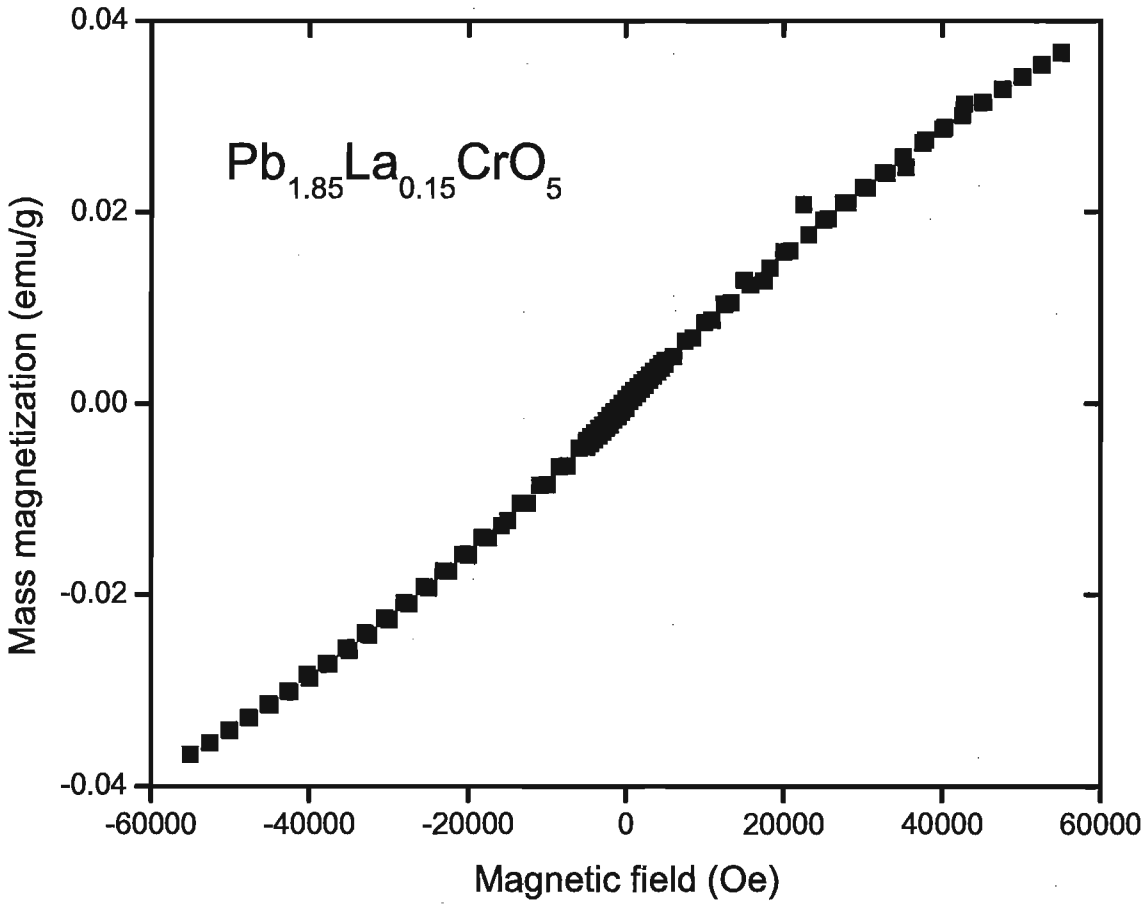

Figure 3.18: **Mass magnetization as a function of the applied magnetic field**

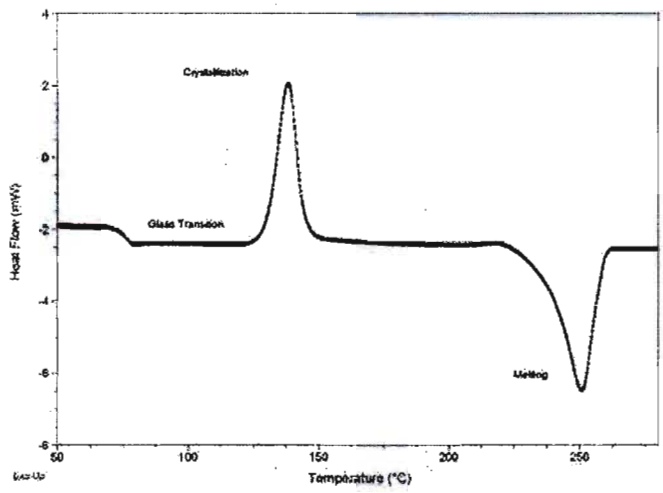

Figure 3.19: **Differential Scanning Calorimetry** [4]

in air with a rate of 2 °C/min. First the sample was cooled down to -50 °C and then DSC was measured as a function of temperature. The mass for the Pb_2CrO_5 sample was 10 mg, for the $Pb_{1.85}La_{0.15}CrO_5$ was 15 mg, and for the $Pb_{1.95}K_{0.05}CrO_5$ it was 8.5 mg. The DSC result for the Pb_2CrO_5 sample is shown in figure 3.20 and we observe an endothermic peak at 9 °C or 282 K. The temperature of this transition is one degree different from the temperature of the magnetization transition that begins at 283 K, as discussed in section 3.2.2. The DSC result of the $Pb_{1.85}La_{0.15}CrO_5$ ceramic sample is given in figure 3.21. The endothermic transition is observed at 10 °C or 283 K. This temperature is four degrees different than the temperature of the beginning of the magnetization transition in this sample (see 3.2.2). The difference in transition temperatures derived from the two experiments could be due to the different heating and cooling rates and the use of different equipment. This experiment was also conducted on the K doped samples but the transition was observed only in the $Pb_{1.95}K_{0.05}CrO_5$ ceramic sample at temperature of 10 °C or 283 K.

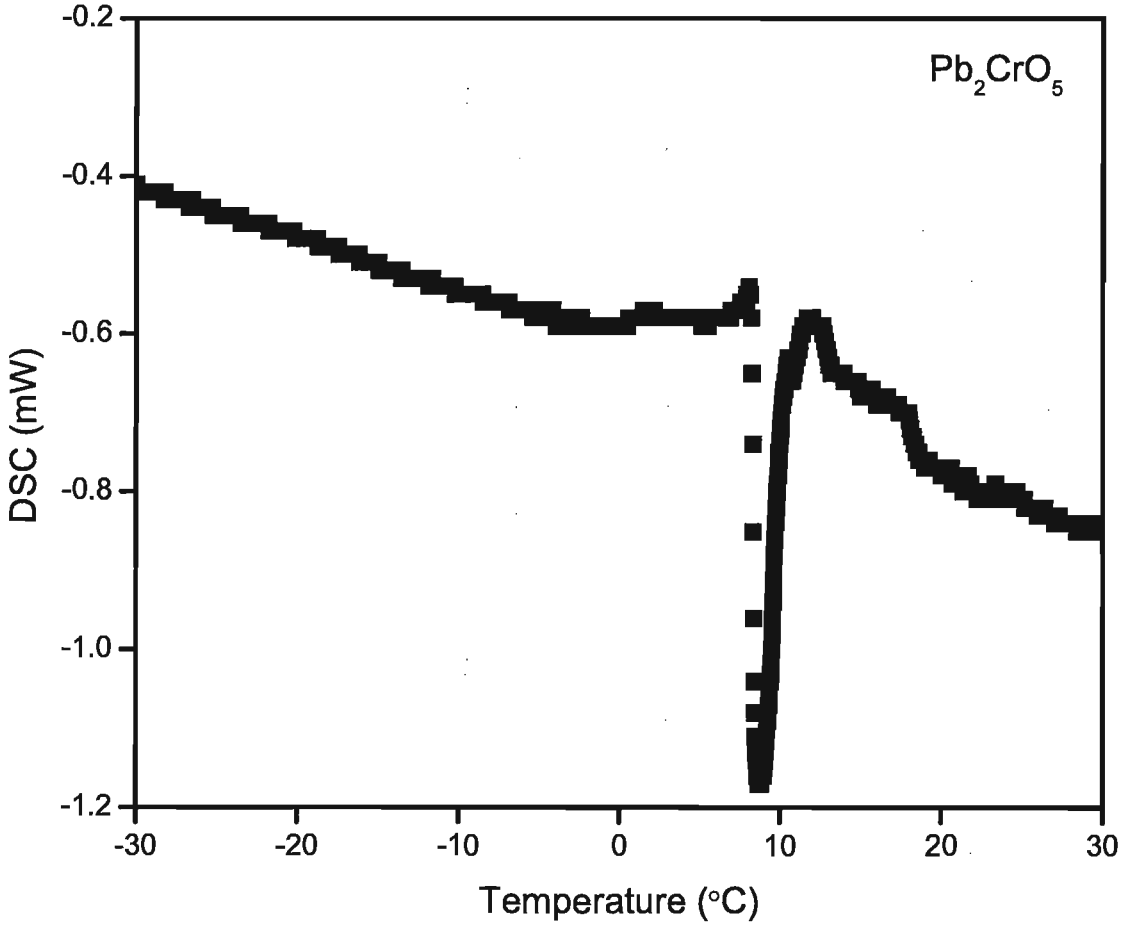

Figure 3.20: **DSC of Pb_2CrO_5 ceramic sample, 2°C/min in air**

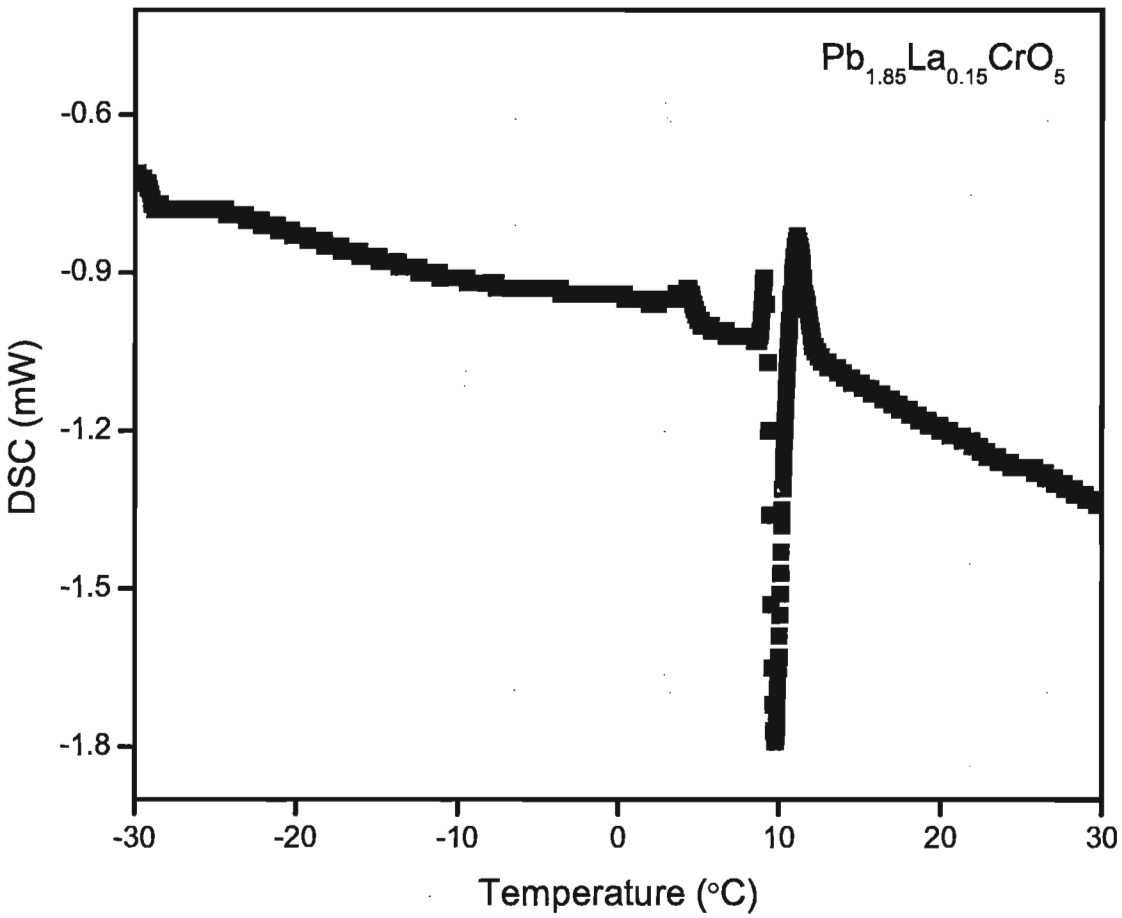

Figure 3.21: **DSC of $Pb_{1.85}La_{0.15}CrO_5$ ceramic sample, 2 °C/min in air**

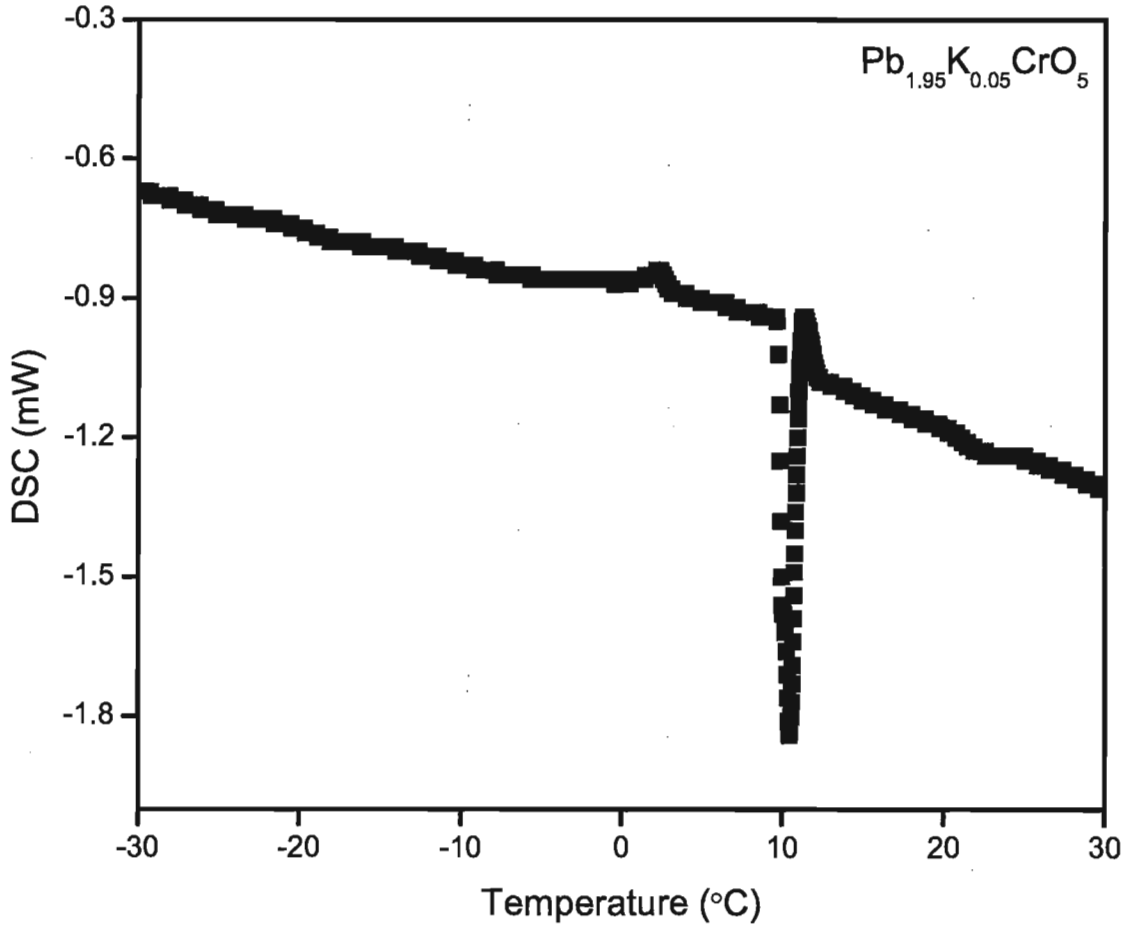

Figure 3.22: **DSC of $Pb_{1.95}K_{0.05}CrO_5$ ceramic sample, 2 °C/min in air**

In conclusion, the Pb_2CrO_5 and $Pb_{1.85}$ $La_{0.15}CrO_5$ samples are showing magnetization transition at about 285 K that has been confirmed with the DSC experiments. K doped samples are undergoing a transition from paramagnetic to diamagnetic state and the transition temperature increases as the amount of K atoms present in the sample is increased. The DSC results are showing that in the $Pb_{1.95}K_{0.05}CrO_5$ sample the transition is observed at about 285 K but it is not present for greater amount of K atoms. The resistivity measurements are indicating a metal-insulator transition near room temperature in the Pb_2CrO_5 sample, where upon increase in temperature the sample becomes ionic conductor. Increase in temperature causes increase in density. This can cause release of the bound valence electrons from the atoms and the electrons become delocalized. This is a transition of material from dielectric to metal, where with the increase in temperature the resistance in sample increases. Once a sufficient temperature is achieved the sample becomes ionic conductor [29].

Chapter 4

Conclusions

Pb_2CrO_5 and K or La doped ceramic samples were prepared using a solid state technique. The crystal structure of these samples was found to be that of the Pb_2CrO_5 Monoclinic C2/m or Pb_2CrO_5, Monoclinic I2/m, but the $Pb_{1.875}K_{0.125}CrO_5$ and $Pb_{1.85}La_{0.15}CrO_5$ samples were found to have impurities. Unannealed and annealed thin films of the parent compound were prepared using the Pulsed Laser Deposition Technique. Using the X ray diffraction technique it was found that the annealing enhances the crystallization of the thin film. The unannealed thin film shows a weak paramagnetism. The paramagnetism is also observed in Pb_2CrO_5 and K or La doped ceramic samples. A decrease of the magnetic moment of the Pb_2CrO_5 sample indicates a magnetization transition beginning near 283 K. In the La doped sample the beginning of the transition is at about 287 K and the magnetic moment drops with greater magnitude. The samples doped with K show a transition from the paramagnetic to the diamagnetic state and the paramagnetism and the transition temperature increases as we increase the amount of dopant. The thermal properties of these samples near room temperature were investigated using the Differential Scanning Calorimetry Technique. Pb_2CrO_5, $Pb_{1.85}La_{0.15}CrO_5$, and $Pb_{1.95}K_{0.05}CrO_5$ show endothermic transitions at about 285 K. This temperature is a few degrees different from the temperatures at which the beginning of the transitions is observed in the magnetization measurements of the parent and La doped samples. The endothermic peak reveals that the samples absorb energy in these transitions. Resistance of the

Pb_2CrO_5 sample was measured as a function of temperature and reveals a gigantic increase in the range between 300 K and 500 K indicating an existence of a metal-insulator transition. Doping the samples with K or La atoms decreases the resistance of the samples. The energy gap of the Pb_2CrO_5 sample was calculated from the resistance experiment to be 1.97 eV.

Appendix A

X ray data

In this appendix we are comparing the values for 2Θ and the intensity for the Pb_2CrO_5 sample that are obtained from the X ray powder diffraction experiment, to the values from the PDF cards for the Pb_2CrO_5 compound: Monoclinic C2/m and Monoclinic I2/m.

Pb_2CrO_5		Pb_2CrO_5, C2/m [15]		Pb_2CrO_5, I2/m [20]	
2Θ (degree)	I (a.u)	2Θ (degree)	I (a.u)	2Θ (degree)	I (a.u)
13.60	379	13.69	162	13.70	160
14.50	286	14.82	135	14.82	120
20.02	355	19.98	131	19.99	130
23.26	340	23.45	80	23.48	90
26.16	1000	26.25	999	26.27	1000
29.78	807	29.90	976	29.92	800
31.38	496	31.46	350	31.50	350
36.00	355	36.16	140	36.19	160
39.70	389	39.75	125	39.75	160
43.48	697	43.94	200	43.96	200
48.61	428	48.67	203	48.68	190
51.50	335	51.55	74	51.57	110
52.70	364	52.92	109	52.97	110
55.04	340	55.18	91	55.20	40

Table A.1: X ray powder diffraction of Pb_2CrO_5 sample

Bibliography

[1] Mineralogy database, 1997-2010, David Barthelmy Web-site: http://webmineral.com/data/phoenicochroite.shtml.

[2] M. Jansen W. Klein. Refinement of the crystal structure of dilead oxide chromate. *Z. Kristallogr. NCS*, pages 219–220, 2010.

[3] Web-site: www.commons.wikimedia.org/wiki/file:edx-scheme.srg.

[4] http://www.npl.co.uk/advanced-materials/measurement-techniques/thermal-analysis/differential-scanning-calorimetry.

[5] Keith Frye. *Mineral Science- An Introductory Survey.* Macmillan Inc., 1993.

[6] K. Toda S. Morita. Determination of the crystal structure of Pb_2CrO_5. *J. Appl. Phys.*, (**55**), 1984.

[7] K. Toda S. Morita. Photoconductivity in a Pb_2CrO_5 ceramic disk with surface electrodes. *Appl. Phys.*, (**33**):231–233, 1984.

[8] S. Yoshida K. Toda. Photovoltaic mechanism of Pb_2CrO_5 ceramic disk with a pair of planar electrodes. *J. Appl. Phys.*, (**63**), 1988.

[9] K. Toda S. Morita. Optical properties and photovoltaic effect in Pb_2CrO_5 thin films. *J. Appl. Phys.*, (**57**):5325–5329, 1985.

[10] K. Toda S. Morita. Preparation of Pb_2CrO_5 thin films by an Electron-Beam Evaporation Technique. *Appl. Phys.*, (**36**), 1985.

[11] S. Watanabe K. Toda. An ultraviolet detector using a Pb_2CrO_5 thin film. *Journal of materials science letters*, (**18**):689–690, 1999.

[12] K. Toda S. Morita. The photoconductive effect in Pb_2CrO_5 thin films prepared by an Electron-Beam Evaporation Technique. *Appl. Phys.*, (**38**):103–107, 1985.

[13] K. Toda S. Yoshida, T. Gyoji. Position-sensitive photodetector using interdigital electrodes on Pb_2CrO_5 thin films. *Int. J. Electronics*, 68:525–531, 1990.

[14] http://www.cpp14.ac.uk/cpp/web-mirrors/crush/astaff/holland/unitcell.html.

[15] Pb_2CrO_5, PDF Card -01-084-0678.

[16] T. Hezareh. Study on the properties of piezoelectric materials and manganese-based oxide perovskites. Master's thesis, Brock University, 2005.

[17] *Coherent User manual COMPexPro® (RoHS)*, 2008.

[18] Rolf Woldseth. *X-ray Energy Spectrometry.* Kevex Corporation, 1 edition, 1973.

[19] B. D. Cullity and S. R. Stock. *Elements of X-ray diffraction.* Prentice-Hall, Inc., 2001.

[20] Pb_2CrO_5, PDF Card -00-029-0768.

[21] Charles Kittel. *Introduction to Solid State Physics.* Wiley, 1971.

[22] $Pb_5O_4(CrO_4)$, PDF Card -01-074-4246.

[23] $Cr_{1.01}LaO_x$, PDF Card -00-044-0333.

[24] Course notes, Advanced Condensed Matter Physics, 5P70.

[25] Charles Kittel. *Introduction to Solid State Physics.* John Wiley & Sons, Inc., 7th edition, 1996.

[26] *MPMS MultiVu Application Users Manual*, 2004.

[27] Mike Mcelfresh. *Fundamentals of Magnetism and Magnetic Measurements*, 1994.

[28] C. Schick. Differential scanning calorimetry (DSC) of semicrystalline polymers. *Anal Bioanal Chem*, (**395**):1589–1611, 2009.

[29] C. N. R. Rao P. P. Edwards. *Metal-Insulator Transitions Revisited.* Taylor & Francis Ltd, 1995.